Title
Angiopoietin-like 4 Is a Wnt Signaling Antagonist that Promotes LRP6 Turnover

Journal
Developmental Cell, 43(1)

ISSN
1534-5807

Authors
Kirsch, Nadine
Chang, Ling-Shih
Koch, Stefan
et al.

Publication Date
2017-10-01

DOI
10.1016/j.devcel.2017.09.011

Peer reviewed

Article

Developmental Cell

Angiopoietin-like 4 Is a Wnt Signaling Antagonist that Promotes LRP6 Turnover

Highlights

- ANGPTL4 is a Wnt signaling antagonist that binds syndecans
- ANGPTL4 promotes turnover of the Wnt co-receptor LRP6
- ANGPTL4 is a Spemann organizer gene in *Xenopus* and promotes notochord development

Authors

Nadine Kirsch, Ling-Shih Chang, Stefan Koch, ..., Maria D.J. Benitez, Edward M. De Robertis, Christof Niehrs

Correspondence

niehrs@dkfz-heidelberg.de

In Brief

Kirsch et al. identify ANGPTL4 as an antagonist of the Wnt/β-catenin signaling pathway. ANGPTL4 binds syndecans to induce internalization and lysosomal degradation of the Wnt co-receptor LRP6, thereby inhibiting Wnt/β-catenin signaling. In *Xenopus* embryos, *angptl4* is expressed in the Spemann organizer and antagonizes Wnt to promote notochord development.

Kirsch et al., 2017, Developmental Cell *43*, 71–82
October 9, 2017
https://doi.org/10.1016/j.devcel.2017.09.011

CellPress

Developmental Cell
Article

Angiopoietin-like 4 Is a Wnt Signaling Antagonist that Promotes LRP6 Turnover

Nadine Kirsch,[1] Ling-Shih Chang,[1] Stefan Koch,[1,4] Andrey Glinka,[1] Christine Dolde,[1,5] Gabriele Colozza,[2] Maria D.J. Benitez,[2] Edward M. De Robertis,[2] and Christof Niehrs[1,3,6,*]
[1]Division of Molecular Embryology, DKFZ-ZMBH Alliance, Deutsches Krebsforschungszentrum (DKFZ), 69120 Heidelberg, Germany
[2]Howard Hughes Medical Institute and Department of Biological Chemistry, University of California, Los Angeles, CA 90095-1662, USA
[3]Institute of Molecular Biology (IMB), 55128 Mainz, Germany
[4]Present address: Department of Clinical and Experimental Medicine (IKE), Linköping University, S-581 85 Linköping, Sweden
[5]Present address: Institute for Cell Biology, University of Bern, 3012 Bern, Switzerland
[6]Lead Contact
*Correspondence: niehrs@dkfz-heidelberg.de
https://doi.org/10.1016/j.devcel.2017.09.011

SUMMARY

Angiopoietin-like 4 (ANGPTL4) is a secreted signaling protein that is implicated in cardiovascular disease, metabolic disorder, and cancer. Outside of its role in lipid metabolism, ANGPTL4 signaling remains poorly understood. Here, we identify ANGPTL4 as a Wnt signaling antagonist that binds to syndecans and forms a ternary complex with the Wnt co-receptor Lipoprotein receptor-related protein 6 (LRP6). This protein complex is internalized via clathrin-mediated endocytosis and degraded in lysosomes, leading to attenuation of Wnt/β-catenin signaling. *Angptl4* is expressed in the Spemann organizer of *Xenopus* embryos and acts as a Wnt antagonist to promote notochord formation and prevent muscle differentiation. This unexpected function of ANGPTL4 invites reinterpretation of its diverse physiological effects in light of Wnt signaling and may open therapeutic avenues for human disease.

INTRODUCTION

The Wnt/β-catenin signaling pathway controls numerous developmental processes and is implicated in stem cell biology and human disease (Holland et al., 2013; Zhan et al., 2016). Wnt ligands bind to LRP5/6 and Frizzled family transmembrane receptors, which triggers a signaling cascade that inhibits GSK3 to stabilize β-catenin. This transcriptional activator then translocates to the nucleus, where it binds to the lymphoid enhancer factor/T cell factor (LEF/TCF) and activates Wnt target genes (MacDonald and He, 2012; Niehrs, 2012). Wnts can engage various co-receptors and relevant for this study are syndecan transmembrane proteoglycans, which negatively regulate Wnt/β-catenin signaling (Astudillo et al., 2014). At the receptor level, Wnt signaling is tightly controlled by secreted antagonists such as Cerberus, Frzb/sFRP3, Dkk1, 2, 4, and Wif1, which inhibit either Wnt ligands or their receptors (Cruciat and Niehrs, 2013). For example, the Wnt signaling antagonist Dkk1 binds to LRP5/6 and induces receptor internalization (Mao et al., 2001, 2002). Conversely, secreted Wnt agonists of the R-spondin family increase surface levels of Frizzled and LRP6 by preventing Wnt receptor ubiquitination and surface clearance (Binnerts et al., 2007; Hao et al., 2012).

In this study, we identify Angiopoietin-like 4 (ANGPTL4) as a Wnt inhibitor. ANGPTL4 belongs to a family of secreted glycoproteins consisting of eight members, whose cellular functions and mechanism of action remain incompletely understood (Santulli, 2014; Zhu et al., 2012). ANGPTL4 is involved in a variety of biological processes. The best-characterized role of ANGPTL4 is the regulation of lipid metabolism. ANGPTL4 attenuates the clearance of circulating triglycerides by inhibition of lipoprotein lipase (Lei et al., 2011; Sukonina et al., 2006; Yoshida et al., 2002), which makes this cytokine a key effector in, e.g., cardiovascular disease and metabolic disorder, and renders it a potential drug target (Dewey et al., 2016; Hato et al., 2008; Kersten, 2005). Moreover, ANGPTL4 is linked to cancer development and metastasis (Nakayama et al., 2011; Padua et al., 2008; Tan et al., 2012), but its molecular function in these disorders is largely unknown.

Here, we describe ANGPTL4 as a Wnt signaling antagonist and show that it inhibits canonical Wnt signaling in mammalian cells and in *Xenopus* embryos. ANGPTL4 binds to syndecans and triggers their endocytosis along with the Wnt co-receptor LRP6, which becomes degraded. In *Xenopus* embryos, *angptl4* is prominently expressed in the Spemann organizer and notochord, where it is required to attenuate Wnt activity to promote notochord development.

RESULTS

ANGPTL4 Is an Inhibitor of Wnt/β-Catenin Signaling

In a genome-wide small interfering RNA (siRNA) screen for Wnt/β-catenin regulators in HEK293T cells (Cruciat et al., 2010; Glinka et al., 2011), we identified ANGPTL4 as a candidate negative regulator. In non-small cell lung cancer H1703 cells, knockdown of *ANGPTL4* by siRNA activated Wnt signaling in β-catenin/TCF reporter assays (TopFlash), while si*ANGPTL3* and si*ANGPTL5* had no effect (Figures 1A, S1A, and S1B). Similarly, si*ANGPTL4* activated Wnt signaling in HEK293T cells, albeit to a lesser extent, and this effect was blocked by addition of exogenous ANGPTL4, supporting specificity (Figure 1B).

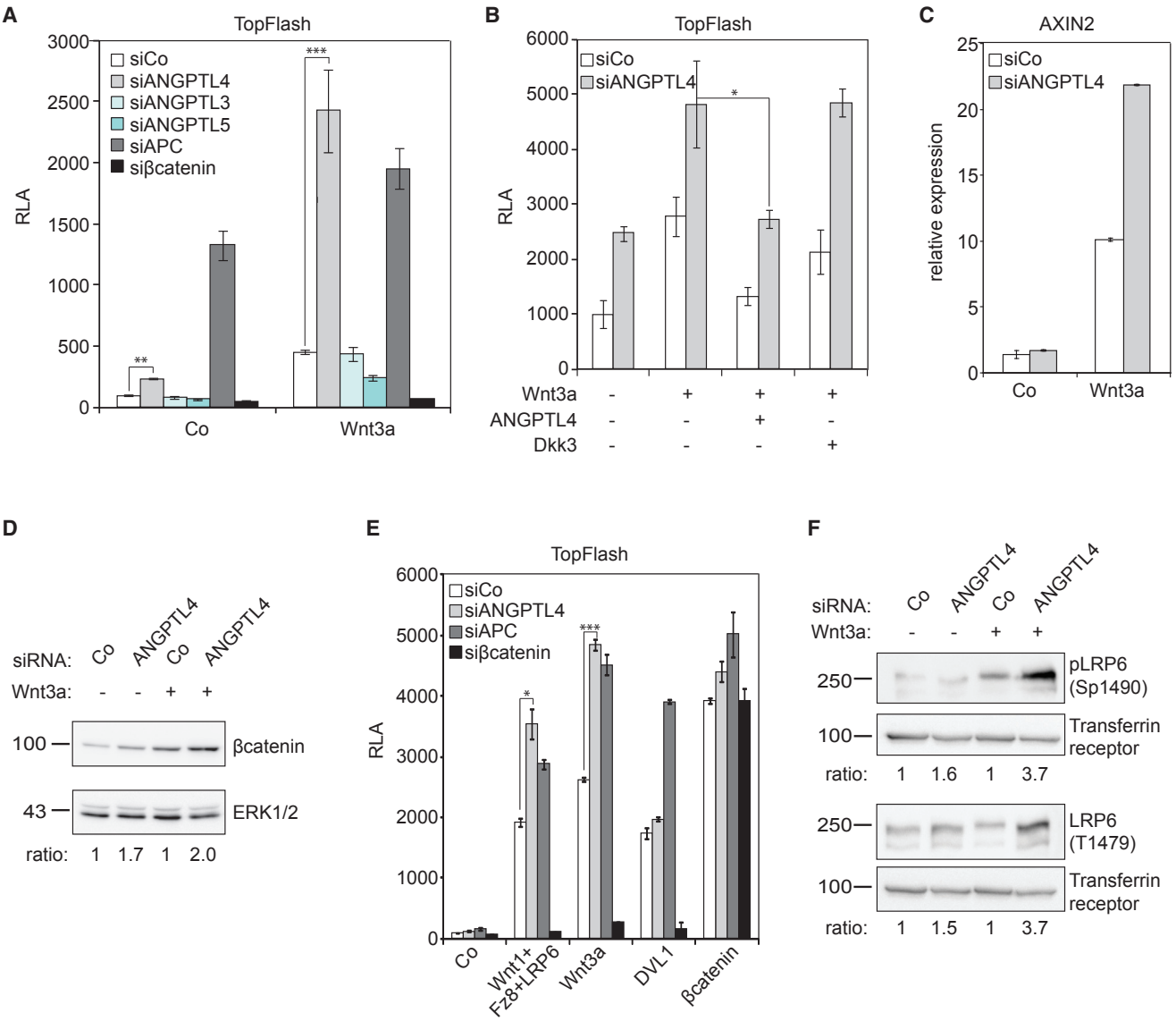

Figure 1. Angiopoietin-like 4 Inhibits Wnt/β-Catenin Signaling at the Receptor Level

(A) Wnt luciferase reporter assay in H1703 cells transfected with the indicated siRNAs, followed by treatment with Wnt3a or control (Co) conditioned medium. si*APC* and si*βcatenin* were included as positive and negative control, respectively.

(B) Wnt reporter assay in HEK293T cells transfected with si*ANGPTL4* or control, followed by treatment with the indicated conditioned media.

(C) qRT-PCR analysis of *AXIN2* expression in H1703 cells transfected with the indicated siRNAs.

(D) Western blot analysis of cytosolic β-catenin in H1703 cells, following transfection with the indicated siRNAs and treatment with control (Co) or Wnt3a conditioned medium.

(E) Wnt reporter epistasis assay in HEK293T cells. Cells were transfected with the indicated plasmids or siRNAs.

(F) Western blot analysis of (activated) phospho-LRP6 in H1703 membrane fractions. Cells were treated with the indicated siRNAs, followed by treatment with Wnt3a or control (Co) conditioned medium.

Data in all graphs are displayed as means ± SD, and show one representative of multiple independent experiments with three biological replicates. RLA, relative luciferase activity. *p < 0.05; **p < 0.01; ***p < 0.001. See also Figure S1.

Consistent with Wnt reporter activation, si*ANGPTL4* strongly induced expression of the Wnt target gene *AXIN2* (Figure 1C) and augmented β-catenin levels (Figure 1D). Moreover, si*ANGPTL4* enhanced Wnt reporter assays stimulated either by a combination of Wnt1, Fz8, and LRP6, or by Wnt3a, but not by downstream components of the pathway, such as Disheveled (DVL1) or β-catenin (Figure 1E), suggesting that ANGPTL4 may act at the level of Wnt receptors. Indeed, depletion of *ANGPTL4* increased protein levels of the Wnt co-receptor LRP6 (Figure 1F), and the magnitude of Wnt reporter activation by si*ANGPTL4* correlated with LRP6 protein levels, i.e., it was high in cells with high LRP6 and *ANGPTL4* levels (H1703, H1299) and lower in cells with low receptor and *ANGPTL4* levels (HEK293T) (Figures S1C–S1I).

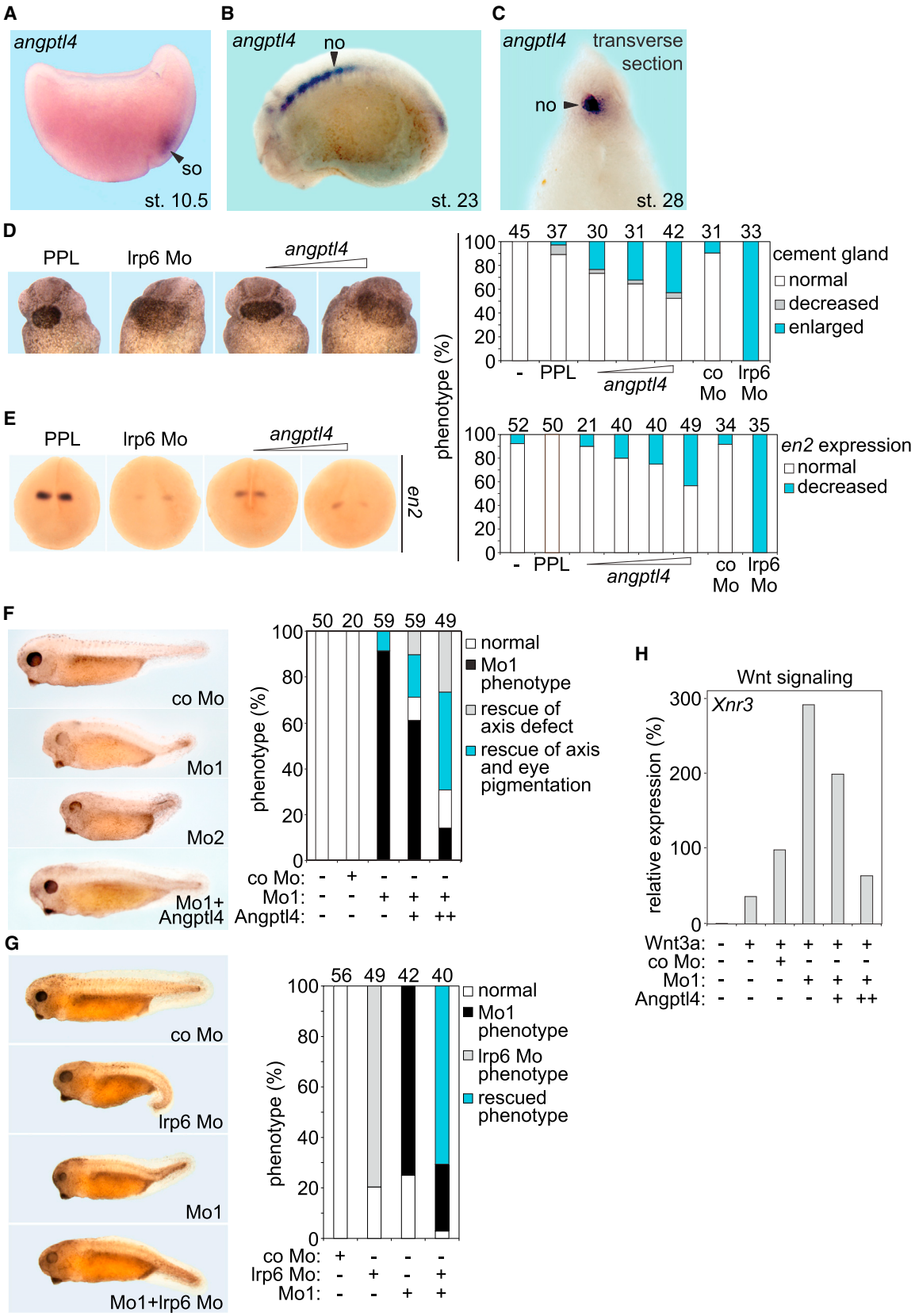

(legend on next page)

ANGPTL4 Inhibits Wnt Signaling in *Xenopus* to Promote Notochord Formation

To investigate the physiological relevance of ANGPTL4-mediated Wnt inhibition, we turned to *Xenopus* embryos, where Wnt signaling prominently regulates early developmental processes. The *Xenopus tropicalis angptl4* homolog was maternally expressed at low levels (Figure S2A, qRT-PCR). Interestingly, data mining revealed that *angptl4* transcripts are highly enriched on the dorsal side of *Xenopus laevis* gastrulae (Figure S2B) and indeed, *angptl4* was expressed in the Spemann organizer (Figure 2A). Since ANGPTL4 inhibits Wnt signaling, this expression domain is particularly revealing since the Spemann organizer is the source of multiple Wnt antagonists, e.g., cerberus, dkk1, and sfrp3/frzb (Bouwmeester et al., 1996; Glinka et al., 1998; Leyns et al., 1997). At later stages, *angptl4* showed highly differential expression in multiple organs during organogenesis (Figure S2C). However, in neurulae and tailbud embryos, *angptl4* expression was largely restricted to the notochord (Figures 2B, 2C, and S2C).

To address the physiological role of *angptl4*, we performed *Xenopus* gain-of-function and loss-of-function experiments. Wnt signaling plays an important role during early *Xenopus* development in mesodermal and anterior-posterior neural patterning (Hoppler et al., 1996; Hoppler and Moon, 1998; Kiecker and Niehrs, 2001). Overexpression of Wnt inhibitors in *Xenopus* embryos typically induces enlarged cement glands and inhibits midbrain development (*en2* expression) (Kiecker and Niehrs, 2001; Leyns et al., 1997). This was also the case when *angptl4* mRNA was microinjected, phenocopying *lrp6* antisense Morpholino oligonucleotide (Mo) injection (Figures 2D and 2E). For loss-of-function, we designed two non-overlapping splice-site antisense Mos (Mo1, Mo2) targeting *angptl4*, microinjection of which strongly reduced endogenous *angptl4* mRNA levels (Figures S2D and S2E). Injection of *angptl4* Mo1 and Mo2 resulted in a similar phenotype, characterized by small heads, shortened bent body axes, and defects in melanocyte and eye pigmentation (Figure 2F). Importantly, co-injection of mouse *Angptl4* mRNA rescued this Mo1 phenotype in a dose-dependent manner (Figure 2F). Moreover, co-injection of *lrp6* Mo also rescued the *angptl4* Mo1 phenotype (Figure 2G), indicating that the malformations are due to elevated Wnt signaling.

There are two phases of Wnt signaling in early *Xenopus* embryos, pre- and post-midblastula transition (MBT), which have the opposite effect on Spemann organizer function. Experimentally, both phases can be distinguished by injection of Wnt RNA versus Wnt DNA, which is expressed only after MBT (Christian and Moon, 1993). Pre-MBT Wnt signaling induces the Spemann organizer and marker genes such as *Xnr3*. Post-MBT Wnt signaling inhibits Spemann organizer and its derivatives (Christian and Moon, 1993; Hoppler et al., 1996; Hoppler and Moon, 1998). *Angptl4* Mo1 enhanced the expression of the Wnt target gene *Xnr3*, a marker for Nieuwkoop center, pre-MBT Wnt signaling. This effect was rescued by co-injection of mouse *Angptl4* mRNA as well (Figure 2H), further corroborating Mo specificity and the inhibitory role of Angptl4 in Wnt signaling.

Notochord formation requires inhibition of post-MBT Wnt signaling to prevent mesodermal precursors from undergoing muscle differentiation (Hoppler et al., 1996; Hoppler and Moon, 1998). Thus, if Angptl4 is a *bona fide* Wnt inhibitor acting in notochord, its loss-of-function should result in a switch from notochord to muscle fate. Indeed, depletion of *angptl4* with either Morpholino reduced the notochord marker *chordin*, as assessed by whole-mount *in situ* hybridization at early neurula stage, phenocopying *Wnt8* DNA gain of function (Figure 3A). Moreover, in animal cap explants induced to form notochord by activin treatment, depletion of *angptl4* with either Morpholino reduced the expression of the notochord/dorsal mesodermal markers *noggin* and *goosecoid* (*gsc*), while inducing the muscle marker *myf5*, similar to *Wnt8* overexpression (Figures 3B and 3C). Corroborating these findings, *angptl4* Mo1 increased *myf5* expression in gastrulae and neurulae, as did *Wnt8* gain-of-function (Figures 3D and 3E, quantified in Figures S3A and S3B). In line with this, *angptl4* mRNA increased the notochord marker *Xnot2* (Figure 3F, quantified in Figure S3C), whereas the muscle marker *myf5* was decreased (Figure 3G, quantified in Figure S3D). This effect was rescued by activation of the Wnt signaling pathway via co-injection of *Wnt8* DNA (Figures 3F and 3G, quantified in Figures S3C and S3D).

Taken together, these results support a model in which *Xenopus* Angptl4 acts as a spatially restricted Wnt antagonist that maintains notochord identity by preventing muscle differentiation.

Figure 2. ANGPTL4 Inhibits Wnt Signaling in *Xenopus*

(A–C) *In situ* hybridization of *angptl4* in *Xenopus* embryos at gastrula (A, *X. laevis,* hemisected dorsal to the right), neurula (B, *X. tropicalis*), and tadpole stage (C, *X. tropicalis*). Sections (A and C) and whole *Xenopus* embryos (B) were used. *Angptl4* expression was largely restricted to Spemann organizer (so) (A) and notochord (no) (B and C).

(D) Cement gland enlargement of tailbud stage *X. laevis* embryos injected with *lrp6* Morpholino (Mo), *angptl4* mRNA, or *PPL* mRNA. The size of the cement gland was analyzed at tailbud (st.23) stage.

(E) Whole-mount *in situ* hybridization of *engrailed 2* (*en2*) in *X. laevis* neurulae. *Xenopus* embryos were injected with *lrp6* Morpholino (Mo), *angptl4* mRNA, or *PPL* mRNA, and *en2* mRNA levels were analyzed at neurula (st.18) stage.

(F) Tadpole stage *X. tropicalis* embryos injected with two different *angptl4* antisense or control (co) Morpholinos (Mo). Where indicated, mouse *Angptl4* mRNA was co-injected. Phenotypes were quantified at tadpole stage by comparing wild-type and Mo-injected embryo morphology and counting embryos with the indicated abnormalities. Axis defects were defined by shortened trunk-tail structures. Mo phenotype: small head, short axis, wavy tail, reduced eye pigmentation, and melanocytes. The number of embryos per condition is indicated on top of the graph.

(G) Tadpole stage *X. tropicalis* embryos injected with *angptl4* Mo1, *lrp6* Mo, or control (co) Mo. Where indicated, *angptl4* Mo1 and *lrp6* Mo were co-injected. Phenotypes were quantified at tadpole stage by comparing wild-type and Mo-injected embryo morphology and counting embryos with the indicated abnormalities. Axis defects were defined by shortened trunk-tail structures.

(H) qRT-PCR analysis of the Wnt target *Xnr3* in animal cap explants at early gastrula (st.10^{+}) from *X. tropicalis* embryos injected with the indicated constructs. Data show one representative of multiple independent experiments with at least three biological replicates. See also Figure S2.

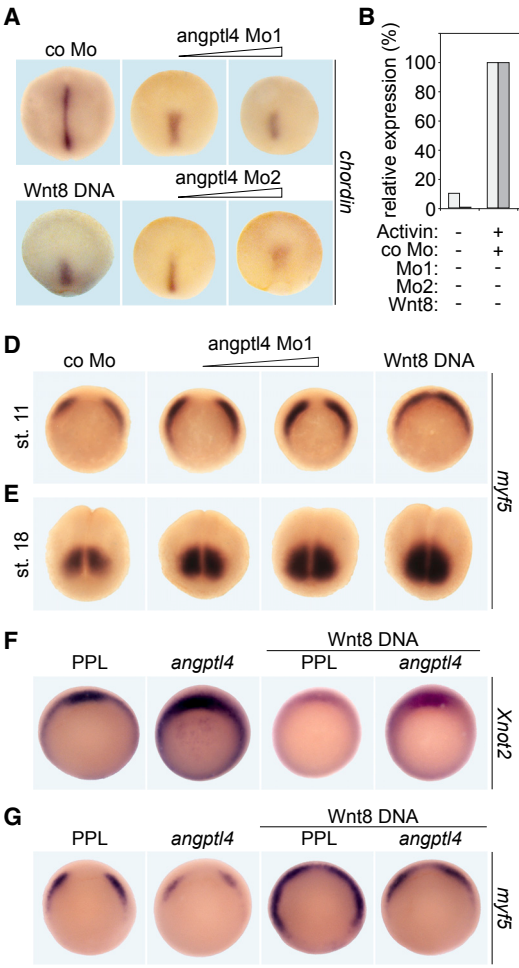

Figure 3. ANGPTL4 Promotes Notochord Formation in *Xenopus*

(A) Whole-mount *in situ* hybridization of *chordin* mRNA at early neurula (st.13). *X. tropicalis* embryos were injected with the indicated Mo or 5 pg *Wnt8* DNA.

(B and C) qRT-PCR analysis of *noggin*, *gsc* (B), and *myf5* (C) in animal cap explants at neurula (st.18) from *X. tropicalis* embryos injected as indicated. Co Mo-injected embryos were set to 100%. Data show one representative of multiple independent experiments with at least three biological replicates.

(D and E) Whole-mount *in situ* hybridization of *myf5* mRNA at gastrula (D, vegetal view, dorsal side top) or neurula (E, posterior view) stage. *X. tropicalis* embryos were injected with *angptl4* Mo1 or *Wnt8* DNA.

(F and G) Whole-mount *in situ* hybridization of *Xnot2* (F, vegetal view, dorsal side top) or *myf5* (G, vegetal view, dorsal side top) mRNA at gastrula stage (st.11). *X. laevis* embryos were injected with *angptl4* mRNA and *PPL* mRNA or in combination with *Wnt8* DNA.

ANGPTL4 Binds to Syndecans

To explore the molecular mechanism by which ANGPTL4 inhibits Wnt signaling, we first determined whether known angiopoietin-like protein interactors are Wnt regulators. Leukocyte immunoglobulin-like receptor B2 (LILRB2) serves as a receptor for ANGPTL2 and ANGPTL5, and it was suggested that it may also bind other ANGPTL proteins (Zheng et al., 2012); however, we did not observe binding of ANGPTL4 to LILRB2 (Figure S4A), and si*LILRB2* had no effect on Wnt signaling (Figure S4B). Likewise, Wnt signaling was not affected by depletion of lipoprotein lipase (LPL) (Figure S4B), which is bound and inhibited by ANGPTL4 (Yoshida et al., 2002). While our results indicated that ANGPTL4 functions in Wnt signaling at the receptor level (Figures 1E and 1F), *in vitro* binding assays failed to support direct binding to either Frizzled or LRP6 (data not shown and see below). In summary, these results suggest that ANGPTL4 controls Wnt signaling via an as yet unknown interaction partner.

We screened for novel ANGPTL4 interactors in HepG2 cells by mass spectrometry following pull-down of soluble ANGPTL4 (Table S1). Intriguingly, among the most prominent hits were syndecans (SDC) 1, 2, and 4. Syndecans are transmembrane proteins that act as co-receptors in various signaling pathways (Tkachenko et al., 2005). In the context of Wnt signaling, syndecans activate the Wnt/PCP pathway (Munoz et al., 2006; Ohkawara et al., 2011) and inhibit Wnt/β-catenin signaling by reducing LRP6 levels (Astudillo et al., 2014). Syndecans can also regulate FGF signaling (Elfenbein and Simons, 2013), but si*ANGPTL4* had no effect on FGF8 reporter assays (Figure S4C). We confirmed binding of ANGPTL4 to SDC in cell-surface binding assays, which showed that soluble ANGPTL4 specifically binds all four syndecan family members (SDC1–4) (Figure 4A). Moreover, in ELISA, alkaline phosphatase (AP)-tagged soluble SDC4 bound dose dependently to immobilized ANGPTL4 (Figure 4B).

Syndecans Internalize ANGPTL4 via Clathrin-Mediated Endocytosis

A characteristic feature of syndecans is their ability to induce endocytosis upon ligand binding (Fuki et al., 1997; Tkachenko and Simons, 2002). We therefore investigated whether ANGPTL4 undergoes SDC-dependent internalization (Figures 4C, S4D, and S4E). Incubation of HepG2 cells with horseradish peroxidase (HRP)-tagged ANGPTL4 at 37°C led to its internalization within 40 min (Figures 4C and S4E). In contrast, no internalization was observed when cells were incubated on ice. Treatment of cells with chlorate to inhibit sulfation of SDC heparan sulfate chains almost completely abrogated ANGPTL4 endocytosis, suggesting that heparan sulfate proteoglycans are required for ANGPTL4 internalization. Simultaneous depletion of all four syndecans using siRNA blocked ANGPTL4 internalization, while depletion of any single syndecan had no effect, indicating that syndecans act redundantly in ANGPTL4 internalization. To determine the endocytic route, cells were treated with inhibitors of clathrin- or caveolin-mediated endocytosis (Figure S4D). The clathrin inhibitor monodansylcadaverine (MDC)

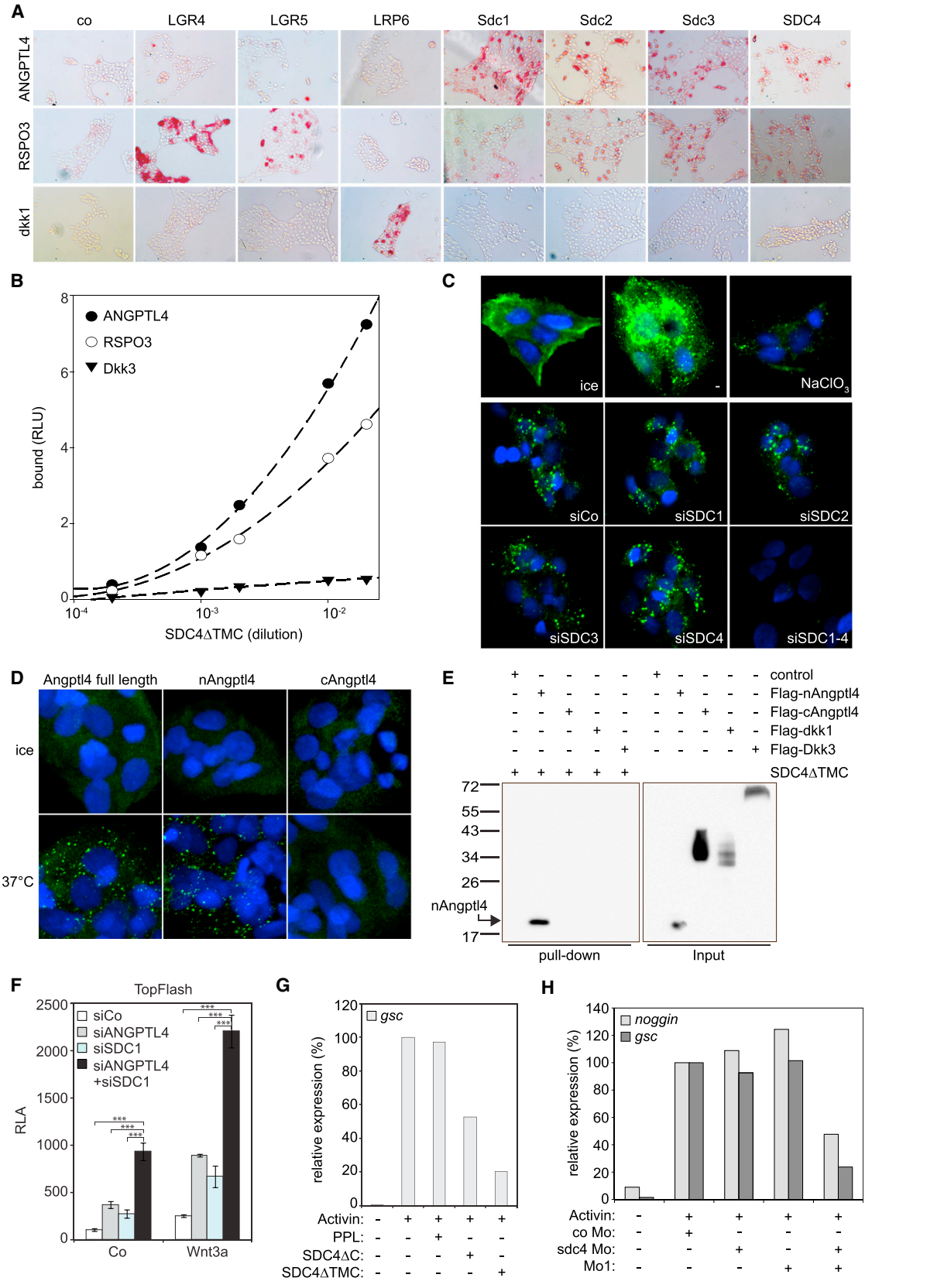

(legend on next page)

blocked ANGPTL4 internalization, unlike inhibitors of caveolin-mediated endocytosis, nystatin and filipin. Concordantly, depletion of *clathrin* by siRNA reduced ANGPTL4 cytoplasmic translocation, whereas si*Caveolin* had no effect (Figure S4D).

N-Terminal Part of ANGPTL4 Is Sufficient for Syndecan Binding

ANGPTL4 is rapidly cleaved upon secretion, and its N- and C-terminal fragments (nANGPTL4 and cANGPTL4, respectively) exert discrete biological functions (Ge et al., 2004; Zhu et al., 2012). Whereas nANGPTL4 is an orphan ligand that mainly controls lipid metabolism, cANGPTL4 binds, e.g., β-integrins, VE-cadherin, and claudin-5 to induce vascular leakiness and tumor progression (Huang et al., 2011; Zhu et al., 2011). We observed that nANGPTL4, but not cANGPTL4, was rapidly internalized in HepG2 cells (Figures 4D and S4F). Likewise, *in vitro* binding assays showed that SDC4 specifically binds nANGPTL4 (Figure 4E). The results corroborate that syndecans bind and internalize nANGPTL4 by clathrin-mediated endocytosis.

In Wnt reporter assays, si*SDC1* and si*ANGPTL4* synergistically activated β-catenin-dependent gene transcription (Figure 4F), indicating that the proteins interact not only biochemically but also functionally. In *Xenopus* explants, injection of dominant-negative SDC4 (SDC4ΔC and SDC4ΔTMC; Ohkawara et al., 2011) reduced the expression of the dorsal mesodermal marker *goosecoid* (*gsc*), whereas the muscle marker *myf5* was induced (Figures 4G and S4G). This phenocopies *angptl4* Mo injection (Figures 3B and 3C) and suggests that ANGPTL4 and syndecans act in the same pathway. Indeed, co-injection of *angptl4* Mo and *sdc4* Mo synergized in reducing notochord/dorsal mesodermal markers *noggin* and *goosecoid* (*gsc*), while synergistically inducing the muscle marker *myf5* (Figures 4H and S4H). This confirms the effects observed *in vitro* and indicates functional interaction of Sdc4 and Angptl4 in *Xenopus* during notochord formation.

ANGPTL4 Promotes LRP6 Turnover

Although we were unable to detect direct binding of ANGPTL4 to LRP6 (Figure 4A), the observation that both syndecans (Astudillo et al., 2014) and ANGPTL4 negatively regulate LRP6 levels raised the possibility that ANGPTL4 controls Wnt signaling by recruiting syndecans to LRP6. To determine if LRP6 and LRP5 are required for the effect of ANGPTL4 on Wnt signaling, we generated LRP6 single and LRP5/6 double knockout HEK293T (HEK293T$^{\Delta LRP5/6}$) cells by CRISPR/Cas9-mediated gene editing (Figure S5A). These cells lack LRP5/6 proteins and are unresponsive to Wnt3a; however they retain the ability to upregulate Wnt signaling upon si*APC* treatment, consistent with a block of Wnt signaling at the receptor level (Figures S5A and S5B). Importantly, in these HEK293T$^{\Delta LRP5/6}$ cells, si*ANGPTL4* depletion failed to induce Wnt reporter activity (Figure 5A). This effect was restored by re-expression of LRP6 in HEK293T$^{\Delta LRP6}$ cells (Figure S5C). Conversely, LRP6 overexpression strongly synergized with si*ANGPTL4* in Wnt reporter induction (Figure 5B). These results confirm the requirement of LRP5/6 for the inhibitory effect of ANGPTL4 on Wnt/β-catenin signaling.

To investigate if ANGPTL4 promotes the association of SDC4 and LRP6, we made use of the proximity ligation assay (PLA). Addition of nANGPTL4 conditioned medium increased the interaction of LRP6 and SDC4, as indicated by the presence of more and larger SDC4-LRP6 clusters in nANGPTL4-treated cells, whereas cANGPTL4 had no effect (Figures 5C, 5D, S5D, and S5E). This LRP6-SDC4 interaction induced by ANGPTL4 was sensitive to chlorate treatment (Figure S5F), suggesting that binding of ANGPTL4 to syndecans is required for LRP6-SDC4 clustering. In *Xenopus* embryos, *angptl4* mRNA reduced LRP6 protein levels, and this effect was reversed by *syndecan 4* Mo (Figure 5E).

In cell-surface biotinylation assays, si*ANGPTL4* increased cell-surface LRP6 without affecting transferrin receptor levels (Figure 5F). Moreover, nANGPTL4 co-localized with LRP6 in endo-/lysosomal vesicles when lysosomal degradation was inhibited with bafilomycin (Figure 5G) or chloroquine (not shown). Taken together, the results support a model in which ANGPTL4 interaction with syndecans promotes the formation of a ternary complex with LRP6, resulting in Wnt receptor clearance and lysosomal degradation. Live-cell imaging of SDC4-LRP6 interaction using a split-fluorescent protein-based bimolecular fluorescence complementation (BIFC) assay (Kodama and Hu, 2010) corroborated this model (Figures 5H and 5I): in untreated cells, addition of nANGPTL4 induced a marked decay of the LRP6-SDC4 BIFC signal (Figure 5H); In contrast, when

Figure 4. Syndecans Are Receptors for nANGPTL4 and Cooperate in Wnt Inhibition

(A) Cell-surface binding assay in HEK293T cells. Cells were transfected with the indicated receptor constructs and treated with conditioned media containing alkaline phosphatase (AP) fusion proteins of ANGPTL4, and the positive control ligands RSPO3ΔC (ligand for LGR4, 5 and SDC1–4) or dkk1 (ligand for LRP6). Ligand binding was detected using a chromogenic AP substrate (red).

(B) ELISA-based *in vitro* binding assay. ANGPTL4, RSPO3ΔC (positive control), and Dkk3 (negative control) were immobilized and incubated with dilutions of alkaline phosphatase (AP)-tagged soluble Syndecan-4 (SDC4ΔTMC). The fraction of bound SDC4 was determined using an AP detection kit.

(C and D) Internalization assay in HepG2 cells. (C) Cells were treated with the indicated siRNAs or sodium chlorate and incubated with HRP-tagged full-length ANGPTL4 (green). (D) Cells were incubated with the indicated myc-tagged Angptl4 constructs. Protein internalization was detected by tyramide signal amplification (C) or anti-myc staining (D).

(E) *In vitro* binding assay of Streptag-HA-SDC4ΔTMC with Flag-tagged Angptl4 N terminus (nAngptl4), C terminus (cAngptl4), dkk1, or Dkk3 recombinant proteins. Pull-down with streptavidin beads shows specific binding of SDC4 to nAngptl4 by immunoblot.

(F) Wnt luciferase reporter assay in H1703 cells stimulated with Wnt3a or control (Co) conditioned medium in the presence of limiting doses of the indicated siRNAs. Data are displayed as means ± SD and show one representative of multiple independent experiments with three biological replicates. RLA, relative luciferase activity. ***$p < 0.001$.

(G and H) qRT-PCR analysis of *gsc* (G, H) and *noggin* (H) in animal cap explants at neurula (st.18) from *X. tropicalis* embryos injected as indicated. Low dose of *angptl4* Mo1 (1 ng) was used in this experiment.

Data show one representative of multiple independent experiments with at least three biological replicates. See also Figure S4 and Table S1.

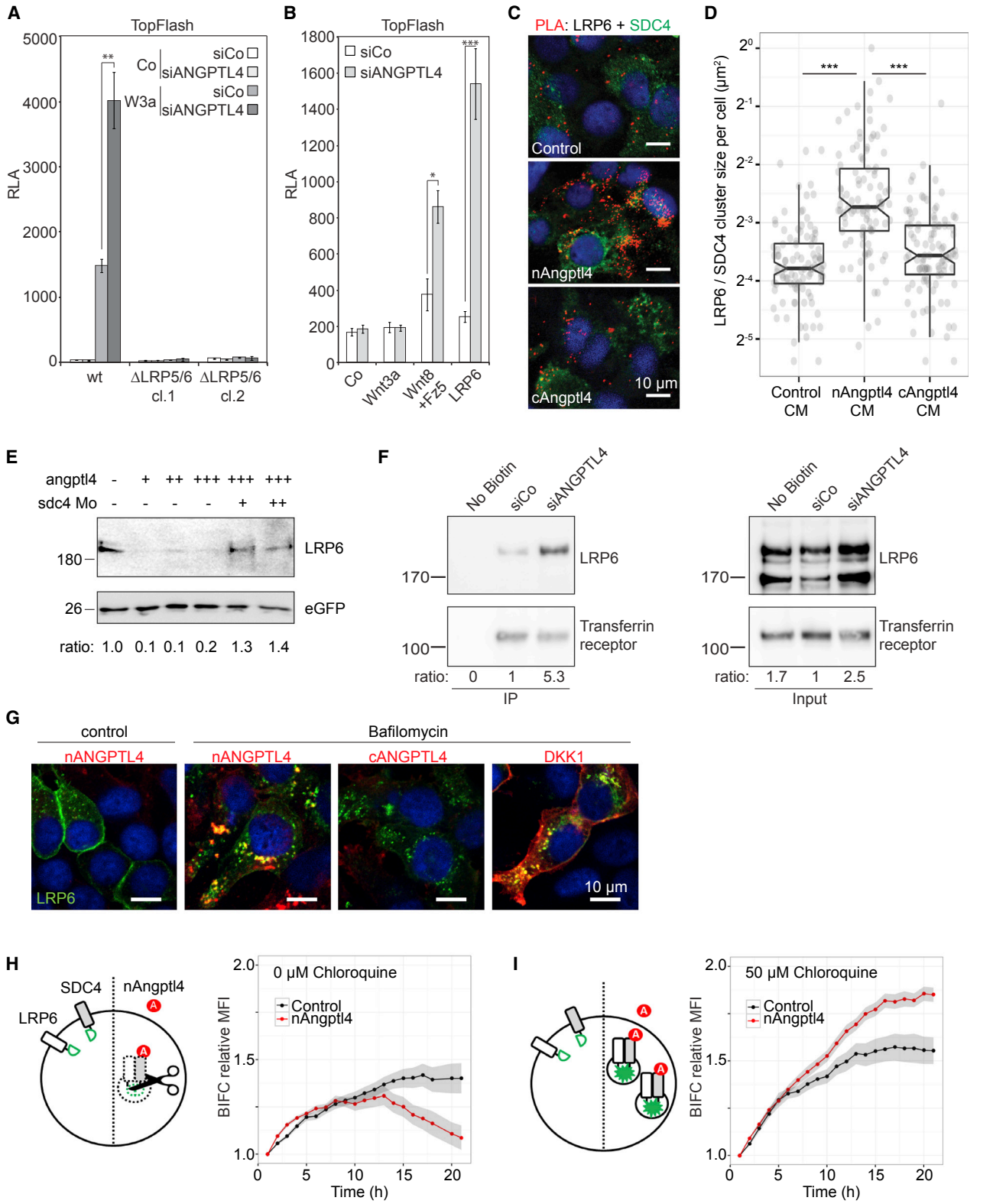

Figure 5. ANGPTL4 Inhibits Wnt Signaling by Decreasing LRP6 Cell Surface Levels

(A) Wnt luciferase reporter assay in parental (wt) and two individual HEK293T$^{\Delta LRP5/6}$ clones transfected with the indicated siRNAs.

(B) Wnt luciferase reporter assay in HEK293T cells. Cells were transfected with limiting doses of the indicated plasmids and siRNAs. Data in (A and B) are displayed as means ± SD and show one representative of multiple independent experiments with three biological replicates. RLA, relative luciferase activity.

(legend continued on next page)

lysosomal degradation was inhibited using chloroquine, nANGPTL4 strongly increased the BIFC signal (Figure 5I). A control BIFC signal using the fibronectin leucine-rich transmembrane protein 3 (FLRT3) and SDC4 was unaffected by nANGPTL4 (Figure S5G).

DISCUSSION

The three main conclusions of our work are that (1) ANGPTL4 is a Wnt antagonist, which inhibits the Wnt/β-catenin pathway by controlling surface levels of the Wnt co-receptor LRP6; (2) syndecans are nANGPTL4 receptors, which mediate ANGPTL4-induced intracellular signaling; (3) *Angptl4* is expressed in the Spemann organizer of *Xenopus* embryos and acts as a Wnt antagonist to promote notochord formation and prevent muscle differentiation.

ANGPTL4 can be added to the growing list of secreted Wnt regulators (Cruciat and Niehrs, 2013), although its mechanism of action is more complex than those of other Wnt inhibitors. Unlike Dkk1, for example, ANGPTL4 does not directly bind to LRP6, but instead to syndecans, which in turn interact with LRP6. The results indicate that it is the LRP6/syndecan complex that is internalized by ANGPTL4. This mode of action resembles the regulation of non-canonical Wnt signaling by RSPO3, which also binds and internalizes syndecans (Ohkawara et al., 2011). In contrast to ANGPTL4, however, R-spondins activate rather than inhibit the canonical and non-canonical Wnt pathways (Kazanskaya et al., 2004; Ohkawara et al., 2011). Thus, depending on the ligand (ANGPTL4 versus RSPO3), syndecan endocytosis can lead to different Wnt signaling outcomes. Furthermore, syndecans can also regulate, e.g., FGF signaling, which remains unaffected by ANGPTL4. This raises the question of ANGPTL4 specificity. The function of ANGPTL4 as a Wnt inhibitor may be context specific, e.g., may be dependent on additional (co-)receptors or adapter proteins such as Disheveled (Astudillo et al., 2014). Of note, β-catenin signaling is decreased in *Angptl2*$^{-/-}$ mice (Horiguchi et al., 2017), and although the underlying mechanism is unclear, this raises the possibility that different members of the Angptl family may both inhibit or promote Wnt signaling, possibly context dependently.

Xenopus Angptl4 is required to antagonize Wnt signaling during dorsal mesoderm formation, notably the notochord. *Xenopus angptl4* is expressed in the Spemann organizer, one of whose molecular hallmarks is to secrete Wnt signaling inhibitors, and Angptl4 is part of a cocktail that includes, e.g., Cerberus, Dkk1, and sFrp3/Frzb (Cruciat and Niehrs, 2013). However, the dorsal mesodermal role of Angptl4 does not seem to be conserved in other vertebrates. Zebrafish, chick, and mouse embryos do not express *Angptl4* in the notochord (see https://zfin.org; http://geisha.arizona.edu; http://www.informatics.jax.org). Moreover, mice mutant for *Angptl4* are viable (Desai et al., 2007; Koster et al., 2005), although some unaccounted embryonic lethality has been observed (Perdiguero et al., 2011). Thus, the situation appears similar to, e.g., R-spondin 2 (Rspo2), which is an evolutionary conserved Wnt effector (Kazanskaya et al., 2004), but where the specific role of *rspo2* during *Xenopus* somitogenesis is also not conserved in mouse (Nam et al., 2007).

With regard to lipid metabolism, our observations outline an additional mode of regulation by ANGPTL4. The ANGPTL4 N-terminus binds and inhibits LPL, thereby controlling triglyceride levels (Lichtenstein et al., 2007). LPL is sequestered on the cell surface by heparan sulfate proteoglycans, including syndecans (Williams, 2009), and it has recently been proposed that inhibition of LPL occurs at the level of the plasma membrane (Chi et al., 2015). In line with this model, we now show that syndecans bind nANGPTL4 as well. Thus, syndecans may act as co-receptors for the ANGPTL4-LPL interaction and thereby facilitate LPL inhibition.

Finally, while we demonstrate physiological significance by showing that ANGPTL4-mediated Wnt inhibition is critical for notochord development in *Xenopus*, our results likely have broader pathobiological implications. First, ANGPTL4 is strongly associated with cancer progression (Padua et al., 2008); however, its function in tumor growth and metastasis has remained controversial due to the complex biological effects of the individual ANGPTL4 domains and its poorly understood mechanism of action (reviewed in Tan et al., 2012). Given the prominent role of Wnt signaling in cancer (Clevers and Nusse, 2012), our findings invite re-assessment of the contribution of ANGPTL4 to the pathogenesis of Wnt-addicted tumors. Second, ANGPTL4 expression strongly correlates with higher triglyceride (TG) levels, and hence the protein is considered a promising target for treating coronary artery disease (CAD) (Dewey et al., 2016; Helgadottir

(C and D) Proximity ligation assay (PLA) in HEK293T$^{\Delta LRP6}$ cells. (C) Cells transfected with V5-LRP6 and SDC4-eYFP were treated with the indicated conditioned media, and LRP6/SDC4 clustering was detected by proximity ligation. Scale bar, 10 μm. (D) Average cluster size in 100 cells per condition was determined by computer-assisted particle analysis. Data are displayed as box and whisker plots with median, interquartile range, and maximum/minimum values excluding outliers. Notches indicate the 95% confidence interval. Tukey's post-hoc test following one-way ANOVA was used for analysis.

(E) Western blot analysis of LRP6 in *X. laevis* animal cap explants at neurula (st.18). mRNAs injected (ng per embryo) were 0.25, 0.5, 1.0 *angptl4*, 0.3 *LRP6*, 0.1 *mMesd*, and 0.1 *eGFP*. *Sdc4* Mo was injected at 20 or 40 ng per embryo.

(F) Cell-surface biotinylation assay in H1703 cells. Cells were transfected with the indicated siRNAs, and surface levels of LRP6 were determined by immunoblot after streptavidin pull-down following biotinylation. Transferrin receptor was used as control. The relative levels of LRP6, normalized to siControl, are indicated below.

(G) Co-immunolocalization assay in HEK293T$^{\Delta LRP6}$ cells. Cells were transfected with LRP6-eGFP (green) and treated as indicated. Flag-tagged ligand was detected by tyramide signal amplification (red). Scale bar, 10 μm.

(H and I) Bimolecular fluorescence complementation (BIFC) assay in H2B-Cerulean HEK293 cells. A schematic presentation of the investigated mechanism is shown on the left. Cells were transfected with SDC4ΔC-C-Venus and LRP6ΔC-N-Venus. LRP6/SDC4 clustering was monitored by fluorescence microscopy, quantifying Venus fluorescence over a field of cells and normalizing to Cerulean fluorescence. Cells were treated with Flag-nAngptl4 or control conditioned medium in the absence (H) or presence (I) of 50 μM chloroquine. For each condition, cells from nine different positions were measured in a time range of 22 hr. Graphs show average relative MFI (mean normalized fluorescence intensity) ± SEM (gray).

*p < 0.05; **p < 0.01; ***p < 0.001. See also Figure S5.

et al., 2016; Myocardial Infarction and Investigators, 2016). Interestingly, LRP6 regulates lipid metabolism as well, and inactivating mutations in LRP6 are similarly linked to elevated TG levels and CAD (Go et al., 2014; Srivastava et al., 2015). ANGPTL4 and syndecans may thus regulate TG metabolism via LRP6. Our results provide new mechanistic insight into the function of a key metabolic and cancer regulator, and may open therapeutic approaches for cardiovascular diseases and cancers.

STAR★METHODS

Detailed methods are provided in the online version of this paper and include the following:

- KEY RESOURCES TABLE
- CONTACT FOR REAGENT AND RESOURCE SHARING
- EXPERIMENTAL MODEL AND SUBJECT DETAILS
  - Cell Lines
  - Animals
- METHOD DETAILS
  - Expression Constructs
  - Cell Culture and Luciferase Reporter Assays
  - Membrane and Cytosolic Cell Extraction
  - Gene Set Analysis
  - *Xenopus* Methods
  - ANGPTL4 Pull-down for MS Analysis
  - Cell-Surface Binding
  - *In Vitro* Binding Assay
  - Streptavidin Pull-down Assay
  - Cell Surface Biotinylation
  - Tyramide Signal Amplification
  - Proximity Ligation Assay (PLA)
  - BIFC Assay
- QUANTIFICATION AND STATISTICAL ANALYSIS
  - Particle Analysis
  - Data Analysis

SUPPLEMENTAL INFORMATION

Supplemental Information includes five figures and one table and can be found with this article online at https://doi.org/10.1016/j.devcel.2017.09.011.

AUTHOR CONTRIBUTIONS

N.K., S.K., A.G., L.-S.C., and C.D. planned, performed, and analyzed the experiments. C.N. supervised the project. N.K., S.K., and C.N. wrote the paper with input from all authors. G.C., M.D.J.B., and E.M.D.R. independently discovered that *angptl4* was an anteriorizing gene in *Xenopus* and provided the Spemann organizer data.

ACKNOWLEDGMENTS

We thank C. Reinhard for technical support; C. Cruciat, D. Ingelfinger, and M. Boutros for siRNA screen cooperation; S. Depner for help in creation of the 293-Cerulean reporter line; D. Dvornikov for help in establishing live imaging; and the Hu lab for providing BIFC constructs. Expert technical support by the DKFZ core facility for light microscopy, the central animal laboratory, and the ZMBH Core Facility for Mass Spectrometry & Proteomics is gratefully acknowledged. We thank Dr. G. Roth and Aska Pharmaceuticals Tokyo for generously providing hCG. This work was supported by grants from the DFG (SFB 873) to C.N. and the HHMI to E.M.D.R.

Received: November 8, 2016
Revised: August 25, 2017
Accepted: September 13, 2017
Published: October 9, 2017

REFERENCES

Astudillo, P., Carrasco, H., and Larrain, J. (2014). Syndecan-4 inhibits Wnt/beta-catenin signaling through regulation of low-density-lipoprotein receptor-related protein (LRP6) and R-spondin 3. Int. J. Biochem. Cell Biol. *46*, 103–112.

Binnerts, M.E., Kim, K.A., Bright, J.M., Patel, S.M., Tran, K., Zhou, M., Leung, J.M., Liu, Y., Lomas, W.E., 3rd, Dixon, M., et al. (2007). R-Spondin1 regulates Wnt signaling by inhibiting internalization of LRP6. Proc. Natl. Acad. Sci. USA *104*, 14700–14705.

Bouwmeester, T., Kim, S., Sasai, Y., Lu, B., and De Robertis, E.M. (1996). Cerberus is a head-inducing secreted factor expressed in the anterior endoderm of Spemann's organizer. Nature *382*, 595–601.

Chi, X., Shetty, S.K., Shows, H.W., Hjelmaas, A.J., Malcolm, E.K., and Davies, B.S. (2015). Angiopoietin-like 4 modifies the interactions between lipoprotein lipase and its endothelial cell transporter GPIHBP1. J. Biol. Chem. *290*, 11865–11877.

Christian, J.L., and Moon, R.T. (1993). Interactions between Xwnt-8 and Spemann organizer signaling pathways generate dorsoventral pattern in the embryonic mesoderm of *Xenopus*. Genes Dev. *7*, 13–28.

Clevers, H., and Nusse, R. (2012). Wnt/beta-catenin signaling and disease. Cell *149*, 1192–1205.

Cong, L., Ran, F.A., Cox, D., Lin, S., Barretto, R., Habib, N., Hsu, P.D., Wu, X., Jiang, W., Marraffini, L.A., et al. (2013). Multiplex genome engineering using CRISPR/Cas systems. Science *339*, 819–823.

Cruciat, C.M., and Niehrs, C. (2013). Secreted and transmembrane wnt inhibitors and activators. Cold Spring Harb Perspect. Biol. *5*, a015081.

Cruciat, C.M., Ohkawara, B., Acebron, S.P., Karaulanov, E., Reinhard, C., Ingelfinger, D., Boutros, M., and Niehrs, C. (2010). Requirement of prorenin receptor and vacuolar H+-ATPase-mediated acidification for Wnt signaling. Science *327*, 459–463.

Davidson, G., Wu, W., Shen, J., Bilic, J., Fenger, U., Stannek, P., Glinka, A., and Niehrs, C. (2005). Casein kinase 1 gamma couples Wnt receptor activation to cytoplasmic signal transduction. Nature *438*, 867–872.

Desai, U., Lee, E.C., Chung, K., Gao, C., Gay, J., Key, B., Hansen, G., Machajewski, D., Platt, K.A., Sands, A.T., et al. (2007). Lipid-lowering effects of anti-angiopoietin-like 4 antibody recapitulate the lipid phenotype found in angiopoietin-like 4 knockout mice. Proc. Natl. Acad. Sci. USA *104*, 11766–11771.

Dewey, F.E., Gusarova, V., O'Dushlaine, C., Gottesman, O., Trejos, J., Hunt, C., Van Hout, C.V., Habegger, L., Buckler, D., Lai, K.M., et al. (2016). Inactivating variants in ANGPTL4 and risk of coronary artery disease. N. Engl. J. Med. *374*, 1123–1133.

Ding, Y., Colozza, G., Zhang, K., Moriyama, Y., Ploper, D., Sosa, E.A., Benitez, M.D.J., and De Robertis, E.M. (2017). Genome-wide analysis of dorsal and ventral transcriptomes of the *Xenopus laevis* gastrula. Dev. Biol. *426*, 176–187.

Elfenbein, A., and Simons, M. (2013). Syndecan-4 signaling at a glance. J. Cell Sci. *126*, 3799–3804.

Fuki, I.V., Kuhn, K.M., Lomazov, I.R., Rothman, V.L., Tuszynski, G.P., Iozzo, R.V., Swenson, T.L., Fisher, E.A., and Williams, K.J. (1997). The syndecan family of proteoglycans. Novel receptors mediating internalization of atherogenic lipoproteins in vitro. J. Clin. Invest. *100*, 1611–1622.

Gawantka, V., Delius, H., Hirschfeld, K., Blumenstock, C., and Niehrs, C. (1995). Antagonizing the Spemann organizer: role of the homeobox gene Xvent-1. EMBO J. *14*, 6268–6279.

Ge, H., Yang, G., Huang, L., Motola, D.L., Pourbahrami, T., and Li, C. (2004). Oligomerization and regulated proteolytic processing of angiopoietin-like protein 4. J. Biol. Chem. *279*, 2038–2045.

Glinka, A., Dolde, C., Kirsch, N., Huang, Y.L., Kazanskaya, O., Ingelfinger, D., Boutros, M., Cruciat, C.M., and Niehrs, C. (2011). LGR4 and LGR5 are R-spondin receptors mediating Wnt/beta-catenin and Wnt/PCP signalling. EMBO Rep. *12*, 1055–1061.

Glinka, A., Wu, W., Delius, H., Monaghan, A.P., Blumenstock, C., and Niehrs, C. (1998). Dickkopf-1 is a member of a new family of secreted proteins and functions in head induction. Nature *391*, 357–362.

Go, G.W., Srivastava, R., Hernandez-Ono, A., Gang, G., Smith, S.B., Booth, C.J., Ginsberg, H.N., and Mani, A. (2014). The combined hyperlipidemia caused by impaired Wnt-LRP6 signaling is reversed by Wnt3a rescue. Cell Metab. *19*, 209–220.

Hao, H.X., Xie, Y., Zhang, Y., Charlat, O., Oster, E., Avello, M., Lei, H., Mickanin, C., Liu, D., Ruffner, H., et al. (2012). ZNRF3 promotes Wnt receptor turnover in an R-spondin-sensitive manner. Nature *485*, 195–200.

Hassler, C., Cruciat, C.M., Huang, Y.L., Kuriyama, S., Mayor, R., and Niehrs, C. (2007). Kremen is required for neural crest induction in *Xenopus* and promotes LRP6-mediated Wnt signaling. Development *134*, 4255–4263.

Hato, T., Tabata, M., and Oike, Y. (2008). The role of angiopoietin-like proteins in angiogenesis and metabolism. Trends Cardiovasc. Med. *18*, 6–14.

Helgadottir, A., Gretarsdottir, S., Thorleifsson, G., Hjartarson, E., Sigurdsson, A., Magnusdottir, A., Jonasdottir, A., Kristjansson, H., Sulem, P., Oddsson, A., et al. (2016). Variants with large effects on blood lipids and the role of cholesterol and triglycerides in coronary disease. Nat. Genet. *48*, 634–639.

Holland, J.D., Klaus, A., Garratt, A.N., and Birchmeier, W. (2013). Wnt signaling in stem and cancer stem cells. Curr. Opin. Cell Biol. *25*, 254–264.

Hoppler, S., Brown, J.D., and Moon, R.T. (1996). Expression of a dominant-negative Wnt blocks induction of MyoD in *Xenopus* embryos. Genes Dev. *10*, 2805–2817.

Hoppler, S., and Moon, R.T. (1998). BMP-2/-4 and Wnt-8 cooperatively pattern the *Xenopus* mesoderm. Mech. Dev. *71*, 119–129.

Horiguchi, H., Endo, M., Kawane, K., Kadomatsu, T., Terada, K., Morinaga, J., Araki, K., Miyata, K., and Oike, Y. (2017). ANGPTL2 expression in the intestinal stem cell niche controls epithelial regeneration and homeostasis. EMBO J. *36*, 409–424.

Huang, R.L., Teo, Z., Chong, H.C., Zhu, P., Tan, M.J., Tan, C.K., Lam, C.R., Sng, M.K., Leong, D.T., Tan, S.M., et al. (2011). ANGPTL4 modulates vascular junction integrity by integrin signaling and disruption of intercellular VE-cadherin and claudin-5 clusters. Blood *118*, 3990–4002.

Kazanskaya, O., Glinka, A., del Barco Barrantes, I., Stannek, P., Niehrs, C., and Wu, W. (2004). R-Spondin2 is a secreted activator of Wnt/beta-catenin signaling and is required for *Xenopus* myogenesis. Dev. Cell *7*, 525–534.

Keller, A., Nesvizhskii, A.I., Kolker, E., and Aebersold, R. (2002). Empirical statistical model to estimate the accuracy of peptide identifications made by MS/MS and database search. Anal. Chem. *74*, 5383–5392.

Kersten, S. (2005). Regulation of lipid metabolism via angiopoietin-like proteins. Biochem. Soc. Trans. *33*, 1059–1062.

Kiecker, C., and Niehrs, C. (2001). A morphogen gradient of Wnt/beta-catenin signalling regulates anteroposterior neural patterning in *Xenopus*. Development *128*, 4189–4201.

Kodama, Y., and Hu, C.D. (2010). An improved bimolecular fluorescence complementation assay with a high signal-to-noise ratio. BioTechniques *49*, 793–805.

Koster, A., Chao, Y.B., Mosior, M., Ford, A., Gonzalez-DeWhitt, P.A., Hale, J.E., Li, D., Qiu, Y., Fraser, C.C., Yang, D.D., et al. (2005). Transgenic angiopoietin-like (angptl)4 overexpression and targeted disruption of angptl4 and angptl3: regulation of triglyceride metabolism. Endocrinology *146*, 4943–4950.

Lei, X., Shi, F., Basu, D., Huq, A., Routhier, S., Day, R., and Jin, W. (2011). Proteolytic processing of angiopoietin-like protein 4 by proprotein convertases modulates its inhibitory effects on lipoprotein lipase activity. J. Biol. Chem. *286*, 15747–15756.

Leyns, L., Bouwmeester, T., Kim, S.H., Piccolo, S., and De Robertis, E.M. (1997). Frzb-1 is a secreted antagonist of Wnt signaling expressed in the Spemann organizer. Cell *88*, 747–756.

Lichtenstein, L., Berbee, J.F., van Dijk, S.J., van Dijk, K.W., Bensadoun, A., Kema, I.P., Voshol, P.J., Muller, M., Rensen, P.C., and Kersten, S. (2007). Angptl4 upregulates cholesterol synthesis in liver via inhibition of LPL- and HL-dependent hepatic cholesterol uptake. Arterioscler. Thromb. Vasc. Biol. *27*, 2420–2427.

MacDonald, B.T., and He, X. (2012). Frizzled and LRP5/6 receptors for Wnt/beta-catenin signaling. Cold Spring Harb Perspect. Biol. *4*.

Mao, B., Wu, W., Davidson, G., Marhold, J., Li, M., Mechler, B.M., Delius, H., Hoppe, D., Stannek, P., Walter, C., et al. (2002). Kremen proteins are Dickkopf receptors that regulate Wnt/beta-catenin signalling. Nature *417*, 664–667.

Mao, B., Wu, W., Li, Y., Hoppe, D., Stannek, P., Glinka, A., and Niehrs, C. (2001). LDL-receptor-related protein 6 is a receptor for Dickkopf proteins. Nature *411*, 321–325.

Munoz, R., Moreno, M., Oliva, C., Orbenes, C., and Larrain, J. (2006). Syndecan-4 regulates non-canonical Wnt signalling and is essential for convergent and extension movements in *Xenopus* embryos. Nat. Cell Biol. *8*, 492–500.

Myocardial Infarction Genetics and CARDIoGRAM Exome Consortia Investigators (2016). Coding variation in ANGPTL4, LPL, and SVEP1 and the risk of coronary disease. N. Engl. J. Med. *374*, 1134–1144.

Nakayama, T., Hirakawa, H., Shibata, K., Nazneen, A., Abe, K., Nagayasu, T., and Taguchi, T. (2011). Expression of angiopoietin-like 4 (ANGPTL4) in human colorectal cancer: ANGPTL4 promotes venous invasion and distant metastasis. Oncol. Rep. *25*, 929–935.

Nam, J.S., Park, E., Turcotte, T.J., Palencia, S., Zhan, X., Lee, J., Yun, K., Funk, W.D., and Yoon, J.K. (2007). Mouse R-spondin2 is required for apical ectodermal ridge maintenance in the hindlimb. Dev. Biol. *311*, 124–135.

Niehrs, C. (2012). The complex world of WNT receptor signalling. Nat. Rev. Mol. Cell Biol. *13*, 767–779.

Ohkawara, B., Glinka, A., and Niehrs, C. (2011). Rspo3 binds syndecan 4 and induces Wnt/PCP signaling via clathrin-mediated endocytosis to promote morphogenesis. Dev. Cell *20*, 303–314.

Padua, D., Zhang, X.H., Wang, Q., Nadal, C., Gerald, W.L., Gomis, R.R., and Massague, J. (2008). TGFbeta primes breast tumors for lung metastasis seeding through angiopoietin-like 4. Cell *133*, 66–77.

Perdiguero, E.G., Galaup, A., Durand, M., Teillon, J., Philippe, J., Valenzuela, D.M., Murphy, A.J., Yancopoulos, G.D., Thurston, G., and Germain, S. (2011). Alteration of developmental and pathological retinal angiogenesis in angptl4-deficient mice. J. Biol. Chem. *286*, 36841–36851.

R Core Team. (2016). R: A Language and Environment for Statistical Computing (R Foundation for Statistical Computing).

Santulli, G. (2014). Angiopoietin-like proteins: a comprehensive look. Front. Endocrinol. *5*, 4.

Schneider, C.A., Rasband, W.S., and Eliceiri, K.W. (2012). NIH Image to ImageJ: 25 years of image analysis. Nat. Methods *9*, 671–675.

Sobotta, M.C., Liou, W., Stocker, S., Talwar, D., Oehler, M., Ruppert, T., Scharf, A.N., and Dick, T.P. (2015). Peroxiredoxin-2 and STAT3 form a redox relay for H2O2 signaling. Nat. Chem. Biol. *11*, 64–70.

Srivastava, R., Zhang, J., Go, G.W., Narayanan, A., Nottoli, T.P., and Mani, A. (2015). Impaired LRP6-TCF7L2 activity enhances smooth muscle cell plasticity and causes coronary artery disease. Cell Rep. *13*, 746–759.

Subramanian, A., Tamayo, P., Mootha, V.K., Mukherjee, S., Ebert, B.L., Gillette, M.A., Paulovich, A., Pomeroy, S.L., Golub, T.R., Lander, E.S., et al. (2005). Gene set enrichment analysis: a knowledge-based approach for interpreting genome-wide expression profiles. Proc. Natl. Acad. Sci. USA *102*, 15545–15550.

Sukonina, V., Lookene, A., Olivecrona, T., and Olivecrona, G. (2006). Angiopoietin-like protein 4 converts lipoprotein lipase to inactive monomers and modulates lipase activity in adipose tissue. Proc. Natl. Acad. Sci. USA *103*, 17450–17455.

Tan, M.J., Teo, Z., Sng, M.K., Zhu, P., and Tan, N.S. (2012). Emerging roles of angiopoietin-like 4 in human cancer. Mol. Cancer Res. *10*, 677–688.

Tkachenko, E., Rhodes, J.M., and Simons, M. (2005). Syndecans: new kids on the signaling block. Circ. Res. *96*, 488–500.

Tkachenko, E., and Simons, M. (2002). Clustering induces redistribution of syndecan-4 core protein into raft membrane domains. J. Biol. Chem. *277*, 19946–19951.

Williams, K.J. (2009). Some things just have to be done in vivo: GPIHBP1, caloric delivery, and the generation of remnant lipoproteins. Arterioscler. Thromb. Vasc. Biol. *29*, 792–795.

Wu, W., Glinka, A., Delius, H., and Niehrs, C. (2000). Mutual antagonism between dickkopf1 and dickkopf2 regulates Wnt/beta-catenin signalling. Curr. Biol. *10*, 1611–1614.

Yoshida, K., Shimizugawa, T., Ono, M., and Furukawa, H. (2002). Angiopoietin-like protein 4 is a potent hyperlipidemia-inducing factor in mice and inhibitor of lipoprotein lipase. J. Lipid Res. *43*, 1770–1772.

Zhan, T., Rindtorff, N., and Boutros, M. (2016). Wnt signaling in cancer. Oncogene *36*, 1461.

Zheng, J., Umikawa, M., Cui, C., Li, J., Chen, X., Zhang, C., Huynh, H., Kang, X., Silvany, R., Wan, X., et al. (2012). Inhibitory receptors bind ANGPTLs and support blood stem cells and leukaemia development. Nature *485*, 656–660.

Zhu, P., Goh, Y.Y., Chin, H.F., Kersten, S., and Tan, N.S. (2012). Angiopoietin-like 4: a decade of research. Biosci. Rep. *32*, 211–219.

Zhu, P., Tan, M.J., Huang, R.L., Tan, C.K., Chong, H.C., Pal, M., Lam, C.R., Boukamp, P., Pan, J.Y., Tan, S.H., et al. (2011). Angiopoietin-like 4 protein elevates the prosurvival intracellular O2(-):H2O2 ratio and confers anoikis resistance to tumors. Cancer Cell *19*, 401–415.

STAR★METHODS

KEY RESOURCES TABLE

REAGENT or RESOURCE	SOURCE	IDENTIFIER
Antibodies		
Mouse anti-FLAG	Sigma-Aldrich	Cat# F3165; RRID: AB_259529
Rat anti-HA	Roche	Cat# ROAHAHA; RRID: AB_2687407
Rabbit anti-Transferrin receptor	Cell Signaling	Cat# 13113
Rabbit anti-LRP6 (T1479)	Davidson et al., 2005	N/A
Rabbit anti-phospho-LRP6 (Sp1490)	Cell Signaling	Cat# 2568; RRID: AB_2139327
Rabbit anti-LRP5	Thermo Fisher Scientific	Cat# 36-5400; RRID: AB_2533267
Mouse anti-β-catenin	BD	Cat# 610154; RRID: AB_397555
Mouse anti-MAPK (ERK1+ERK2)	Sigma-Aldrich	Cat# M8159; RRID: AB_477245
Mouse anti-Tubulin	Sigma-Aldrich	Cat# T5168; RRID: AB_477579
Anti-GFP	Antibodies-online	Cat# ABIN100085; RRID: AB_10778192
Goat anti-mouse HRP	Jackson ImmunoResearch	Cat# 115-035-146; RRID: AB_2307392
Biological Samples		
Xenopus tropicalis embryos	NASCO	N/A
Xenopus tropicalis embryos	EXRC	N/A
Xenopus tropicalis embryos	CRB	N/A
Xenopus laevis embryos	NASCO	N/A
Chemicals, Peptides, and Recombinant Proteins		
Sephadex beads G-50	Sigma-Aldrich	Cat# 9004-54-0
Streptavidin Agarose	Thermo Fisher Scientific	Cat# 20359
CH-IgG rabbit beads	This paper	N/A
TEV protease	Life Technologies	Cat# 12575-015
Heparin-Agarose	Sigma-Aldrich	Cat# H6508
Bafilomycin A1	Sigma-Aldrich	Cat# 196000
Chloroquine	Sigma-Aldrich	Cat# C6628
Monodansylcadaverine (MDC)	Sigma-Aldrich	Cat# 30432
LightCycler 480 Probes master	Roche	Cat# 04887301001
cOmplete, Protease Inhibitor Cocktail	Roche	Cat# 11873580001
DharmaFECT 1 Transfection Reagent	Dharmacon	Cat#T-2001
X-tremeGENE 9 DNA Transfection Reagent	Roche	Cat#XTG9-RO
LDS sample buffer	Life Technologies	Cat# NP0008
Critical Commercial Assays		
Dual-Luciferase reporter assay system	Promega	Cat# E1960
Chemiluminescent SEAP Reporter Gene Assay	Roche	Cat# 11 779 842 001
Duolink In Situ Detection kit Orange	Sigma-Aldrich	Cat#DUO92007
Duolink In Situ PLA Probe Goat PLUS	Sigma-Aldrich	Cat#DUO92003
Duolink In Situ PLA Probe Rabbit MINUS	Sigma-Aldrich	Cat#DUO92005
Experimental Models: Cell Lines		
HEK293T	GenHunter Corporation	Cat# Q401
HepG2	ATCC	ATCC No. HB-8065
H1703	ATCC	ATCC No. CRL-5889
H1299	ATCC	ATCC No. CRL-5803
L cells stably transfected with mouse Wnt3a	ATCC	ATCC No. CRL-2647
Control L cells (without stably transfected mouse Wnt3a)	ATCC	ATCC No. CRL-2648
HEK293TΔLRP6	This paper	N/A

(*Continued on next page*)

Continued

REAGENT or RESOURCE	SOURCE	IDENTIFIER
HEK293TΔLRP5/6	This paper	N/A
Experimental Models: Organisms/Strains		
Xenopus tropicalis WT	NASCO	N/A
Xenopus tropicalis WT	EXRC	N/A
Xenopus tropicalis WT	CRB	N/A
Xenopus laevis WT	NASCO	N/A
Oligonucleotides		
Primer for Cloning of *X. tropicalis angptl4*: Forward: ATGAAGCTGTTACTTGCAAGTATAACT Reverse: CACAGTAAGGTCTGTATCAACAGG	This paper	N/A
Primer for Cloning of *X. laevis angptl4-l*: Forward: CCGCTCGAGTAAGATGAAGCTGTTATTTGCAAG Reverse: CCGTCTAGAATTCACACCGATAGATCTACATCC	This paper	N/A
Guide RNA for LRP5: GGAAAACTGGAAGTCCACTG	This paper	N/A
Guide RNA for LRP6: ATTATTGTCCCCCGATGGGC	This paper	N/A
Control Morpholino	Standard Control morpholino, Gene Tools	N/A
Morpholino targeting X. tropicalis angptl4 (Mo1): 5'-TTTATCTGACCTGAAAGGTGTTTGG-3'	This paper Gene Tools	N/A
Morpholino targeting X. tropicalis angptl4 (Mo2): 5'-TGTCGGCCACTCACTTGAAACAATA-3'	This paper Gene Tools	N/A
Morpholino targeting Xenopus lrp6	Hassler et al., 2007 Gene Tools	N/A
Morpholino targeting Xenopus sdc4	Munoz et al., 2006 Gene Tools	N/A
siRNA targeting sequence: ANGPTL4	Dharmacon	Cat# M-007807-02
qRT-PCR primer: Xnr3 (UPL probe #102) Forward: CCAAAGCTTCATCGCTAAAAG Reverse: AAAAGAAGGGAGGCAAATACG	Roche	N/A
qRT-PCR primer: noggin (UPL probe #29) Forward: TGGGGAGTTGGATCTCCTT Reverse: TTTGATTTCTGCTGGCATTG	Roche	N/A
qRT-PCR primer: gsc (UPL probe #126) Forward: GAAACCAAGTACCCAGACGTG Reverse: CCTCCACTTTGCTCTTCGAT	Roche	N/A
qRT-PCR primer: myf5 (UPL probe #66) Forward: AGCTGCTCAGATGGCATGA Reverse: AGCTGCTGTTCCTTCCAGAC	Roche	N/A
qRT-PCR primer: angptl4 (UPL probe #88) Forward: TCTGATTTTAACTGCGCCAAA Reverse: ATGGCCGCATGAGCTAAA	Roche	N/A
qRT-PCR primer: angptl4 (UPL probe #21) Forward: TTGAAGTCTATTGTGAAATGACAGC Reverse: CCCAGAGCCGATCAAAATC	Roche	N/A
Recombinant DNA		
Mouse Angptl4	Source BioScience	IMAGE ID 5137159
Human ANGPTL4	Source BioScience	IMAGE ID 5088323
Software and Algorithms		
EZ-C1 software v3.80	Nikon Corporation	N/A
Excellence rt 2.0 Software	Olympus Soft Imaging Solutions GmbH	N/A
Mascot software	Matrix Science, version 2.4.1.	N/A
Scaffold (Proteome Software, version 4.7.5)	http://www.proteomesoftware.com/products/scaffold/	N/A

(*Continued on next page*)

Continued		
REAGENT or RESOURCE	SOURCE	IDENTIFIER
R 3.3.1	R Core Team, 2016	N/A
Fiji (ImageJ)	https://fiji.sc/	N/A
Other		
Nunc Lab-Tek Chambered Coverglass, 8-well	Thermo Fisher Scientific	Cat# 155411

CONTACT FOR REAGENT AND RESOURCE SHARING

Further information and requests for resources and reagents should be directed to and will be fulfilled by the Lead Contact, Christof Niehrs (niehrs@dkfz-heidelberg.de).

EXPERIMENTAL MODEL AND SUBJECT DETAILS

Cell Lines

HEK293T are female and HepG2 are male. Both cell lines were cultivated under standard conditions in DMEM, 10% FCS, 1% penicillin/streptomycin (10.000 U/ml), and 1% L-glutamine (200 mM) at 37°C in a humidified atmosphere with 10% CO_2 unless otherwise indicated. H1703 and H1299 cell lines are male and were grown in RPMI, 10% FCS, 1% penicillin/streptomycin (50 μg/ml), 1% L-glutamine (200 mM) and 1% sodium pyruvate (11 mg/ml) at 37°C in a humidified atmosphere with 5% CO_2 unless otherwise indicated. L cells are male and were cultivated in DMEM, 10% FCS, 1% penicillin/streptomycin (10.000 U/ml), and 1% L-glutamine (200 mM) at 37°C in a humidified atmosphere with 5% CO_2. All cells used are listed in the Key Resources Table.

Animals

All *Xenopus* experiments were approved by the state review board of Baden-Württemberg (Germany) and performed according to federal and institutional guidelines. Frogs were obtained from NASCO, EXRC and CRB and kept in a *Xenopus* facility designed by Tecniplast. *Xenopus laevis* are kept at 18°C and *Xenopus tropicalis* at 25°C with a light/dark cycle of 12 h/12 h.

Females were injected with 600 U (*X. laevis*) or 10 U followed by 200 U within 1-5 days (*X. tropicalis*) of Human Chorionic Gonadotropin (hCG) from Aska. Males were killed by keeping in high dose of anesthetic MS222 dissolved in water. Only adult, mature males and females were used to obtain sperms and eggs, respectively. For all experiments only embryos were used at the indicated stage. Embryos were injected with Morpholino or mRNA as indicated in the method details and figure legends.

METHOD DETAILS

Expression Constructs

Mouse and human ANGPTL4 were obtained from Source BioScience (accession No.: BC025797, BC023647). *Xenopus tropicalis angptl4* was cloned from stage 40 *X. tropicalis* embryos using the following primers: 5'ATGAAGCTGTTACTTGCAAGTATAACT, 3'CACAGTAAGGTCTGTATCAACAGG. *Xenopus laevis angptl4-l* was cloned from stage 10.5 using: 5'CCGCTCGAGTAAGAT GAAGCTGTTATTTGCAAG, 3'CCGTCTAGAATTCACACCGATAGATCTACATCC. Epitope-tagged constructs were generated by inserting full length or deleted forms of the respective genes into a pCS-based vector containing an N-terminal myc, Flag or Streptag-HA-HRP tag, or C-terminal AP tag.

Cell Culture and Luciferase Reporter Assays

Wnt luciferase reporter assays in HEK293T, H1703 or H1299 cells were carried out in 96-well plates in 100 μl. For loss-of-function assays, $2x10^5$ HEK293T cells per ml or $1x10^5$ H1299 / H1703 cells per ml were transfected with 50 nM of siRNAs and a non-targeting Control siRNA (Dharmacon) using Dharmafect 1 (Dharmacon) transfection reagent if not otherwise indicated. After 24 h, plasmid DNA was transfected using Xtreme Gene 9 DNA transfection reagent (Roche). A total of 100 ng of DNA was transfected per well, including 10 ng TopFlash, 5 ng pTK-Renilla, 10 ng mWnt1, 2 ng mFz8, 12 ng hLRP6, 0.2 ng *Xenopus* β-catenin, 40 ng hDVL1. pCS2+ DNA was used to adjust total DNA amount to 100 ng per well. After 24 h luciferase activity was determined using the Dual-luciferase reporter assay system (Promega). When cells were stimulated with Wnt3a, control or Wnt3a conditioned medium was added 6 h after plasmid DNA transfection and treatment was proceeded over night. Afterwards luciferase activity was measured (Cruciat et al., 2010; Glinka et al., 2011; Wu et al., 2000). HEK293T$^{\Delta LRP6}$ and HEK293T$^{\Delta LRP5/6}$ cells were generated by CRISPR/Cas9-mediated gene editing (Cong et al., 2013) with the following gRNAs: LRP5: GGAAAACTGGAAGTCCACTG; LRP6: ATTATTGTCCCCCGATGGGC. siRNAs were from Thermo Scientific Dharmacon: si*ANGPTL4*-1: GAAAGAGGCUGCCCGAGAU, si*ANGPTL4*-2: ACAAGCACCUAGAC CAUGA, si*ANGPTL4*-3: GACACAAGCAGGCGCCAAU, si*ANGPTL4*-4: GGGACAAGAACUGCGCCAA, and from Sigma: si*ANGPTL3* and si*ANGPTL5*.

Membrane and Cytosolic Cell Extraction

Subcellular fractionation was performed as follows: Cells were gently scraped into ice-cold Hank's BSS and centrifuged at 200 x g for 5 min at 4°C. Cells were resuspended in 50 µl Saponin buffer (1x TBS, 0.05% Saponin, 1 mM $MgCl_2$, 2 mM β-mercaptoethanol, 10 mM NaF, 5 mM glycerophosphate, 0.1 mM PMSF, 1x complete protease inhibitor cocktail (Roche)), and incubated 30 min on ice. After centrifugation at 17,500 x g for 5 min at 4°C, the supernatant (cytosolic fraction) was boiled in Laemmli buffer. The pellet was resuspended in 50 µl NP-40 lysis buffer (50 mM Tris-HCl pH 7.5, 150 mM NaCl, 10 mM NaF, 1x complete protease inhibitor cocktail (Roche), 1% NP-40, 0.1% SDS, 5 mM β-mercaptoethanol, 5 mM glycerophosphate) and incubated on ice for 30 min. Samples were centrifuged at 10,500 x g for 3 min at 4°C, and the supernatant was incubated in LDS sample buffer (Life Technologies, NP0008) with 10 mM DTT for 10 min at 70°C.

Gene Set Analysis

Gene Set Expression Analysis (GSEA, Subramanian et al., 2005), was carried out using RNA-seq data described elsewhere (Ding et al., 2017).

Xenopus Methods

In vitro fertilization, embryo culture, staging and microinjection at two-to-four cell stage were carried out as described (Gawantka et al., 1995). Based on the *Xenopus tropicalis angptl4* sequence (ENSXETG00000021893), two antisense Morpholino oligonucleotides (Mos) were designed: 5'-TTTATCTGACCTGAAAGGTGTTTGG-3' (Mo1), 5'-TGTCGGCCACTCACTTGAAACAATA-3' (Mo2). The splicing Morpholinos target exon-intron boundaries in exon 6 or 8 of the *angptl4* pre-mRNA sequence, resulting in exon 6 and 8 skipping, respectively. The primers for qRT-PCR target mRNA sequences in exon 6/7: F- TTGAAGTCTATTGTGAAATGACAGC and R-CCCAGAGCCGATCAAAATC to analyze exon 6 skipping induced by Mo2 and mRNA sequences in exon 8/9: F-TCTGATTT TAACTGCGCCAAA and R-ATGGCCGCATGAGCTAAA to analyze exon 8 skipping induced by Mo1.

Equal amounts of total Mo or mRNA were injected by adjustment with the standard control Mo (Gene Tools) or *PPL* mRNA, respectively, where necessary. *Lrp6* Mo (1 or 2 ng) and *sdc4* Mo (5 ng) were used as described (Hassler et al., 2007). The mRNA doses for injections were (pg per embryo): 3 *Wnt3a*, 80 *Activin*, 2 *Wnt8*, 250 or 500 *angptl4*. Whole-mount *in situ* hybridizations were carried out essentially as described (Gawantka et al., 1995). For analysis of notochord and muscle markers using whole-mount *in situ* hybridization, embryos were injected equatorially with 20 or 40 ng *angptl4* Mo, 5 pg, 10 pg or 20 pg *Wnt8* DNA per embryo with respective controls. Embryos were collected at embryonic stage 11 (gastrula), 13 (early neurula), or 18 (neurula) and processed for *in situ* hybridization. For analysis of notochord mRNA levels pictures of *angptl4* morphants were taken together with respective control embryos. The same was done for *Wnt8* DNA injected embryos. Phenotypes were scored using a stereomicroscope by comparing wt and Mo-injected embryo morphology and counting embryos with the indicated abnormalities.

For western blot analysis, *X. laevis* embryos were injected animally with the following mRNAs (ng per embryo): 0.25, 0.5, 1.0 *angptl4*, 0.3 *LRP6*, 0.1 *mMesd*, and 0.1 *eGFP*. *Sdc4* Mo was injected at 20 or 40 ng per embryo. Animal cap explants were collected at neurula (st.18) and homogenized in NP-40 lysis buffer (2% NP-40, 20 mM Tris-HCl pH 7.5, 150 mM NaCl, 10 mM NaF, 10 mM Na_3VO_4, 10 mM sodium pyrophosphate, 5 mM EDTA, 1 mM EGTA, 1 mM PMSF, and protease inhibitors (Roche)) at one explant per 3 µl. Homogenates were extracted with Freon and analyzed by SDS-PAGE.

ANGPTL4 Pull-down for MS Analysis

HepG2 cells were seeded in 15 cm-dishes and medium was changed after 24 h. Two days after seeding $ProteinA_{x2}$-TEV-Streptag-HRP-hANGPTL4 conditioned medium was added to cells. After 30 min at 37°C, medium was removed and cells were washed, lysed in 5 ml ice cold lysis buffer (1% Triton X-100, 2 mM β-mercaptoethanol, 1 mM $MgCl_2$, 1x complete protease inhibitor cocktail (Roche), 1x TBS, pH 7.5) for 10 min on ice and Dounce homogenization performed. After centrifugation the supernatant was supplemented with 1 mM EDTA and EGTA to avoid precipitation of the proteins. After a pre-clearing step using Sephadex beads, lysates were incubated with IgG beads overnight with rotation at 4°C. The following day beads were washed and ANGPTL4 was eluted overnight at 4°C using TEV protease. After elution, ANGPTL4 was bound to Streptavidin beads (Thermo Fisher, 20359). Binding to beads proceeded overnight at 4°C with rotation. Beads were washed and ANGPTL4 was eluted several times by addition of 2 mM Biotin. Eluted proteins were separated by SDS-PAGE and stained with Coomassie Blue. Each lane was cut into four gel pieces. After in-gel trypsin digestion peptides were analyzed by LC-MSMS on an Orbitrap Elite (Thermo Scientific) as described (Sobotta et al., 2015). For database search with the Mascot software (Matrix Science, version 2.4.1.) the human uniprot database with 20348 entries was used. Data were evaluated by Scaffold (proteome software, version 4.7.5). Protein identifications were accepted with a minimum of two identified peptides (minimum of 95% probability by the peptide prophet algorithm (Keller et al., 2002)).

Cell-Surface Binding

Recombinant protein conditioned media were produced by transient transfection of HEK293T cells with hRSPO3ΔC-AP, Xdkk1-AP and hANGPTL4-AP in complete DMEM (10% FBS, 1% Glutamine, 1% Penicillin-Streptomycin) at 32°C. ANGPTL4-AP was partially purified from conditioned medium via heparin agarose beads (Sigma-Aldrich, Type I), washed with TBS, and eluted with 0.5 M NaCl and 20 mM Tris (pH 7.5). Eluted protein was dialyzed against TBS. For cell surface binding assays, HEK293T cells were seeded one day before transfection on Poly-L-Lysine-treated 24-well plates, that they reached 50% confluence at the day of transfection. Cells were transfected with 200 ng of the indicated plasmid DNA using Xtreme Gene 9 (Roche) transfection reagent. After 48 h cells were

incubated with conditioned media for 2 h on ice, washed with ice cold Hank's buffer, fixed for 30 min with 0.5 mM DSP (Pierce) in Hank's with 100 mM HEPES (pH 7.2), washed with 0.1 M Tris (pH 8.0), and stained with Fast Red (Roche) (Ohkawara et al., 2011). For LGR4/5, LRP6, SDC4 human constructs and for Sdc1, 2, 3 mouse constructs were used for transfection.

In Vitro Binding Assay

Recombinant protein conditioned media were produced by transient transfection of HEK293T cells with Streptag-hRSPO3ΔC, Streptag-mDkk3, Streptag-hANGPTL4 and SDC4ΔTMC-AP in complete DMEM. For *in vitro* binding assay, white high-binding ELISA 96-well plates (Greiner) were coated overnight at 4°C with 100 μl of 2 μg/ml Streptavidin in bicarbonate buffer (50 mM $NaHCO_3$, pH 9.6). Wells were washed three times with TBS-T and blocked with 5% BSA in TBS-T on a shaker for 1 h at room temperature. After four additional washing steps with TBS-T, Streptag-hANGPTL4, -hRSPO3ΔC or -mDkk3 conditioned medium was applied in 5% BSA in TBS-T and allowed to bind overnight at 4°C. Wells were washed six times with TBS-T and incubated with different dilutions of AP-tagged SDC4ΔTMC in 5% BSA in TBS-T and 1 mM $MgCl_2$ for 2 h. Wells were washed six times with TBS-T. Bound AP activity was measured using the chemiluminescent SEAP Reporter Gene Assay (Roche). For each dilution, background binding was subtracted.

Streptavidin Pull-down Assay

Recombinant protein conditioned media were produced by transient transfection of HEK293T cells with Streptag-HA-hSDC4ΔTMC, Flag-Xdkk1, Flag-mDkk3, Flag-mAngptl4 N-terminal and C-terminal domain in complete DMEM. Streptag-HA-SDC4ΔTMC was pulled-down at 4°C from conditioned medium using Streptavidin beads (Thermo Fisher, 20359). After 24 h incubation, beads were washed first with wash buffer (1x TBS, 1% Triton X-100, pH 7.5) and afterwards with complete DMEM. Flag-tagged recombinant proteins were applied as conditioned media and binding was carried out at 4°C for 24 h. Beads were washed with complete DMEM and wash buffer and analyzed by SDS-PAGE and Western blotting using anti-HA (Roche, 1867423) and anti-Flag (Sigma-Aldrich, F-3165) antibodies.

Cell Surface Biotinylation

For detection of cell surface proteins, cells were transfected with siRNA for 24 h. Cells were then washed 2x with PBS, and incubated with 0.5 mM NHS-LC-LC-Biotin (Thermo Fisher) in PBS for 30 min on ice with gentle agitation. Cells were blocked with 10 mM monoethanolamine, and washed 3x with 100 mM glycine in PBS, followed by 2x wash with 20 mM glycine. Biotinylated proteins were detected by pull down with streptavidin agarose (Thermo Scientific, 20359), followed by immunoblot with LRP6 (Davidson et al., 2005) and transferrin receptor (Cell Signaling, 13113) antibodies.

Tyramide Signal Amplification

$HEK293T^{\Delta LRP6}$ cells were transfected with LRP6-GFP, SDC4-HA, and MesD for 48 h. Cells were incubated with conditioned media containing Flag-tagged proteins for 4 h at 37°C in the presence of Bafilomycin A1 (Sigma, 250 nM) or Chloroquine (Sigma, 50 μM). Cells were washed with PBS, fixed with 4% PFA, permeabilized w/ 1% Triton X-100, and blocked with 3% BSA in PBS w/ 0.1% Tween-20. Ligands were detected by labelling with mouse anti-Flag and goat anti-mouse HRP antibodies, followed by tyramide-rhodamine reaction as described (Glinka et al., 2011).

Proximity Ligation Assay (PLA)

$HEK293T^{\Delta LRP6}$ cells were transfected with V5-LRP6, SDC4-eYFP, and MesD for 48 h. V5-LRP6/xDvl2-GFP and LRP6-GFP/Flag-Xflrt3 were used as positive and negative control, respectively. In some experiments, 20 mM $NaClO_3$ or NaCl control were added for the entire transfection period. Cells were incubated with conditioned media containing Flag-tagged proteins for 20 min at 37°C. PLA was performed using the Duolink In Situ Detection kit (Sigma), according to the supplier's recommendations. Multiple images per condition were acquired on a Nikon C1 confocal microscope controlled by EZ-C1 software, using identical detector settings.

BIFC Assay

For bimolecular fluorescence complementation (BIFC) assay HEK293 cells stably expressing nuclear Histone H2B-Cerulean were generated as follows: Cells were infected with retrovirus containing Histone H2B-Cerulean fusion under Puromycin resistance and one H2B-Cerulean expressing clone was selected. LRP6 and SDC4 Split Venus constructs were cloned by substituting the intracellular part of LRP6 with N-terminal part of Venus (aa 1-172, I152L mutated) and intracellular part of SDC4 with C-terminal part of Venus (aa 155-238) according to Hu lab recommendations (Kodama and Hu, 2010).

For BIFC assay 50 000 cells per well were seeded in 8 well Chambered Coverglass (Lab-Tek w/cvr #1, 155411, Thermo Scientific) using DMEM without Phenol red, supplemented with 10% FBS. The next day cells were transfected with 5 ng of SDC4ΔC C-Venus and 20 ng LRP6ΔC N-Venus or 20 ng Xflrt3ΔC N-Venus DNA using XtremeGene 9 transfection reagent (Roche). 24 h after transfection Flag-nAngptl4 or control conditioned medium was added to each well with or without 50 μM Chloroquine. Cells were subjected to live cell imaging at 37°C, 5% CO_2 for 24 h using an Olympus CellR IX81microscope with "Excellence rt 2.0" software (Olympus Soft Imaging Solutions GmbH). In each well 9 positions, containing confluent cells, were defined at the beginning of the experiment. At 1 h interval each position was photographed in the blue channel for nuclei (H2B-Cerulean; Ex. 415-455 nm, Em. 460-500 nm) and the

yellow channel (BIFC; Ex. 505-555 nm, Em. 565-630 nm). Images were analyzed using ImageJ 1.49g (Schneider et al., 2012). Fluorescence of an entire frame was quantified and the Venus signal was normalized to the Cerulean signal. The Venus/Cerulean ratio for each frame was then normalized to the Venus/Cerulean ratio of time point 1 for each of the 9 positions.

QUANTIFICATION AND STATISTICAL ANALYSIS

Particle Analysis

Proximity ligation and internalization assays were analyzed by computer-assisted particle analysis in ImageJ. Individual channels were thresholded using the MaxEntropy plugin at default settings, and overlapping particles were separated using the Binary - Watershed function. Dots were counted using the Analyze Particles function at particle size 0.2-5 μm, circularity 0.25-1.

Data Analysis

Data were analyzed using an unpaired two-tailed Student's t-test in Excel 2010 (Microsoft), or one-way analysis of variance (ANOVA), followed by Tukey's or Dunnet's post-hoc test in R 3.3.1 (R Core Team, 2016). Statistically significant results in all figures are indicated as *: $p < 0.05$; **: $p < 0.01$; and ***: $p < 0.001$.

Developmental Cell, Volume *43*

Supplemental Information

Angiopoietin-like 4 Is a Wnt Signaling Antagonist that Promotes LRP6 Turnover

Nadine Kirsch, Ling-Shih Chang, Stefan Koch, Andrey Glinka, Christine Dolde, Gabriele Colozza, Maria D.J. Benitez, Edward M. De Robertis, and Christof Niehrs

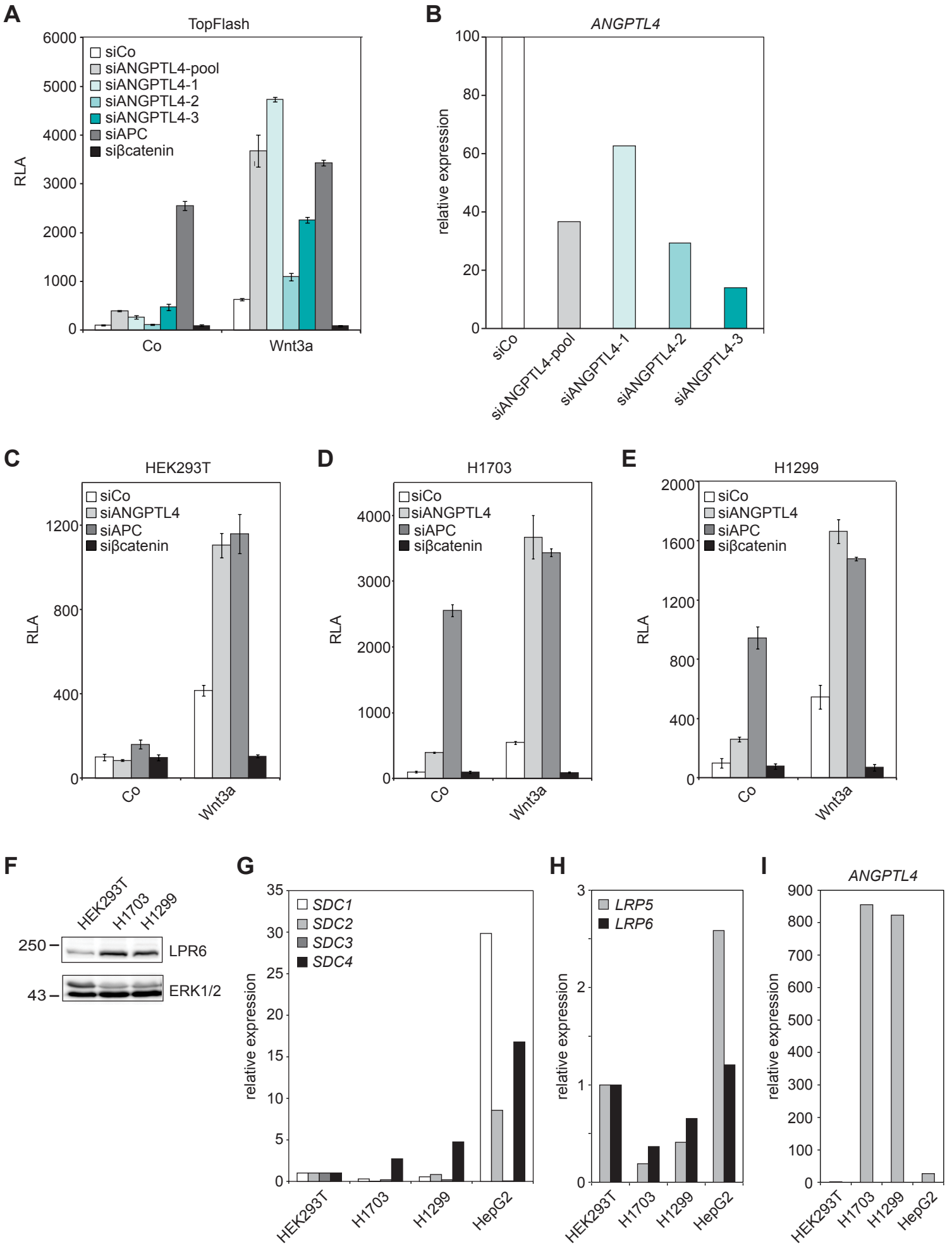
A
TopFlash
RLA
6000
5000
4000
3000
2000
1000
0
siCo
siANGPTL4-pool
siANGPTL4-1
siANGPTL4-2
siANGPTL4-3
siAPC
siβcatenin
Co
Wnt3a
B
ANGPTL4
relative expression
100
80
60
40
20
0
siCo
siANGPTL4-pool
siANGPTL4-1
siANGPTL4-2
siANGPTL4-3
C
HEK293T
RLA
1200
800
400
0
siCo
siANGPTL4
siAPC
siβcatenin
Co
Wnt3a
D
H1703
RLA
4000
3000
2000
1000
0
siCo
siANGPTL4
siAPC
siβcatenin
Co
Wnt3a
E
H1299
RLA
2000
1600
1200
800
400
0
siCo
siANGPTL4
siAPC
siβcatenin
Co
Wnt3a
F
HEK293T
H1703
H1299
250
LPR6
43
ERK1/2
G
relative expression
35
30
25
20
15
10
5
0
SDC1
SDC2
SDC3
SDC4
HEK293T
H1703
H1299
HepG2
H
relative expression
3
2
1
0
LRP5
LRP6
HEK293T
H1703
H1299
HepG2
I
ANGPTL4
relative expression
900
800
700
600
500
400
300
200
100
0
HEK293T
H1703
H1299
HepG2

Figure S1, related to Figure 1. The extent of Wnt inhibition by ANGPTL4 correlates with cellular LRP6 protein levels.

(A) Wnt luciferase reporter assay in H1703 cells stimulated with control or Wnt3a-conditioned medium. Cells were transfected with *ANGPTL4* siRNA SMARTpool (pool) or three individual *ANGPTL4* siRNAs (1, 2, 3). si*APC* and si*βcatenin* were included as positive and negative controls, respectively. Graphs show mean ± SD, *N=3*. Co, control. RLA, relative luciferase activity.

(B) qRT-PCR analysis of *ANGPTL4* to analyze siRNA knockdown efficiencies in H1703 cells used in panel (A).

(C-E) Wnt luciferase reporter assays in HEK293T (C), H1703 (D) and H1299 (E) cells. si*APC* and si*βcatenin* were included as positive and negative controls, respectively. Graphs show mean ± SD, *N=3*. Co, control. RLA, relative luciferase activity.

(F) LRP6 protein levels as analyzed by Western blot in indicated cell lines. ERK1/2 was used as loading control.

(G-I) Expression analysis of *SDC1-4* (G), *LRP5/6* (H) and *ANGPTL4* (I) in HEK293T, H1703, H1299 and HepG2 cells via qRT-PCR.

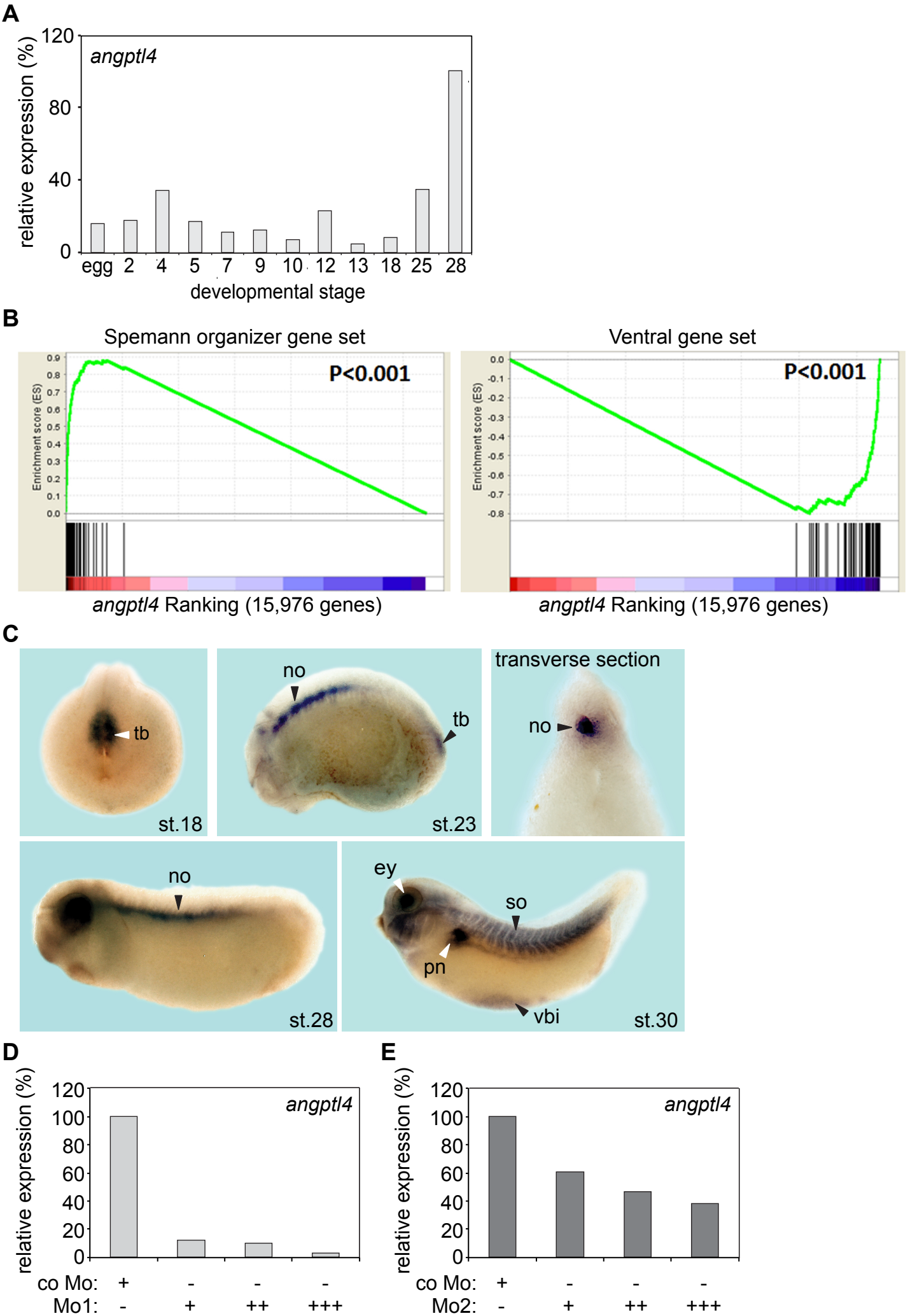
A
angptl4
relative expression (%)
120
80
40
0
egg 2 4 5 7 9 10 12 13 18 25 28
developmental stage
B
Spemann organizer gene set
P<0.001
Enrichment score (ES)
angptl4 Ranking (15,976 genes)
Ventral gene set
P<0.001
Enrichment score (ES)
angptl4 Ranking (15,976 genes)
C
tb
st.18
no
tb
st.23
transverse section
no
no
st.28
ey
so
pn
vbi
st.30
D
angptl4
relative expression (%)
120
100
80
60
40
20
0
co Mo: + - - -
Mo1: - + ++ +++
E
angptl4
relative expression (%)
120
100
80
60
40
20
0
co Mo: + - - -
Mo2: - + ++ +++

Figure S2, related to Figure 2. *Angptl4* is expressed in Spemann organizer, notochord, somites and eye of *Xenopus* embryos.

(A) qRT-PCR analysis of *angptl4* in *X. tropicalis* embryos at different developmental stages. *Ornithine decarboxylase* (*odc*) was used for normalization.

(B) Left, gene Set Expression Analysis (GSEA, Subramanian et al., 2005) showing that a set of 107 *X. laevis* Spemann organizer-specific genes (Ding et al., 2017) strongly correlated with genes from six dorsal-ventral libraries comprising 15,976 genes ranked according to their correlation with *angptl4*. Right panel, a set of 70 ventral lip-specific genes (identified in Ding et al., 2017) was inversely correlated with *angptl4*. This data mining confirms that *angptl4* is expressed in the Spemann organizer, the precursor of the notochord, at early gastrula (st.10.5).

(C) Whole-mount *in situ* hybridization of *angptl4* mRNA in *X. tropicalis* embryos at the indicated stages. Tb, tailbud mesoderm; no, notochord; ey, eye; pn, pronephros; so, somites; vbi, ventral blood island.

(D, E) qRT-PCR analysis of *angptl4* in *X. tropicalis* embryos at stage 11 that were injected with two different *angptl4* antisense splice-site (Mo1 (D), Mo2 (E)) or control (co) Morpholinos (Mo). Two different primer pairs were used to analyze exon skipping of Mo1 or Mo2 respectively.

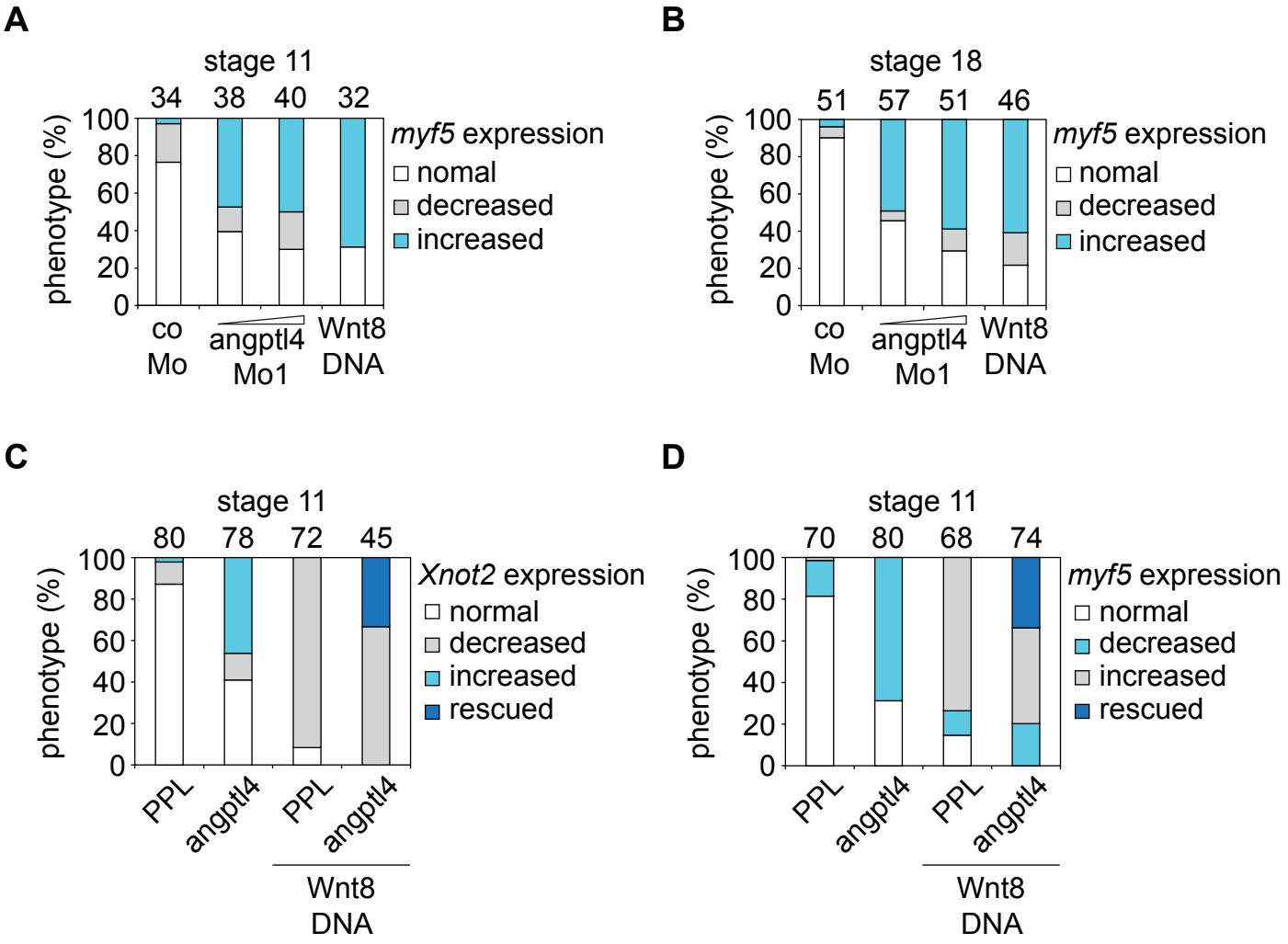
A
stage 11
34 38 40 32
phenotype (%)
100
80
60
40
20
0
co Mo
angptl4 Mo1
Wnt8 DNA
myf5 expression
nomal
decreased
increased
B
stage 18
51 57 51 46
phenotype (%)
co Mo
angptl4 Mo1
Wnt8 DNA
myf5 expression
nomal
decreased
increased
C
stage 11
80 78 72 45
phenotype (%)
PPL
angptl4
PPL
angptl4
Wnt8 DNA
Xnot2 expression
normal
decreased
increased
rescued
D
stage 11
70 80 68 74
phenotype (%)
PPL
angptl4
PPL
angptl4
Wnt8 DNA
myf5 expression
normal
decreased
increased
rescued

Figure S3, related to Figure 3. *Angptl4* increases notochord and decreases muscle marker gene expression in *Xenopus* embryos.

(A, B) Quantification of *myf5* expression by ISH at gastrula (A) and neurula (B) in *angptl4* morphants (related to Fig. 3D and Fig. 3E).

(C, D) Quantification of *Xnot2* (C) and *myf5* (D) expression by ISH at gastrula (st.11) in *X. laevis* embryos injected with *angptl4* mRNA, *PPL* mRNA alone or in combination with *Wnt8* DNA (related to Fig. 3F and Fig. 3G).

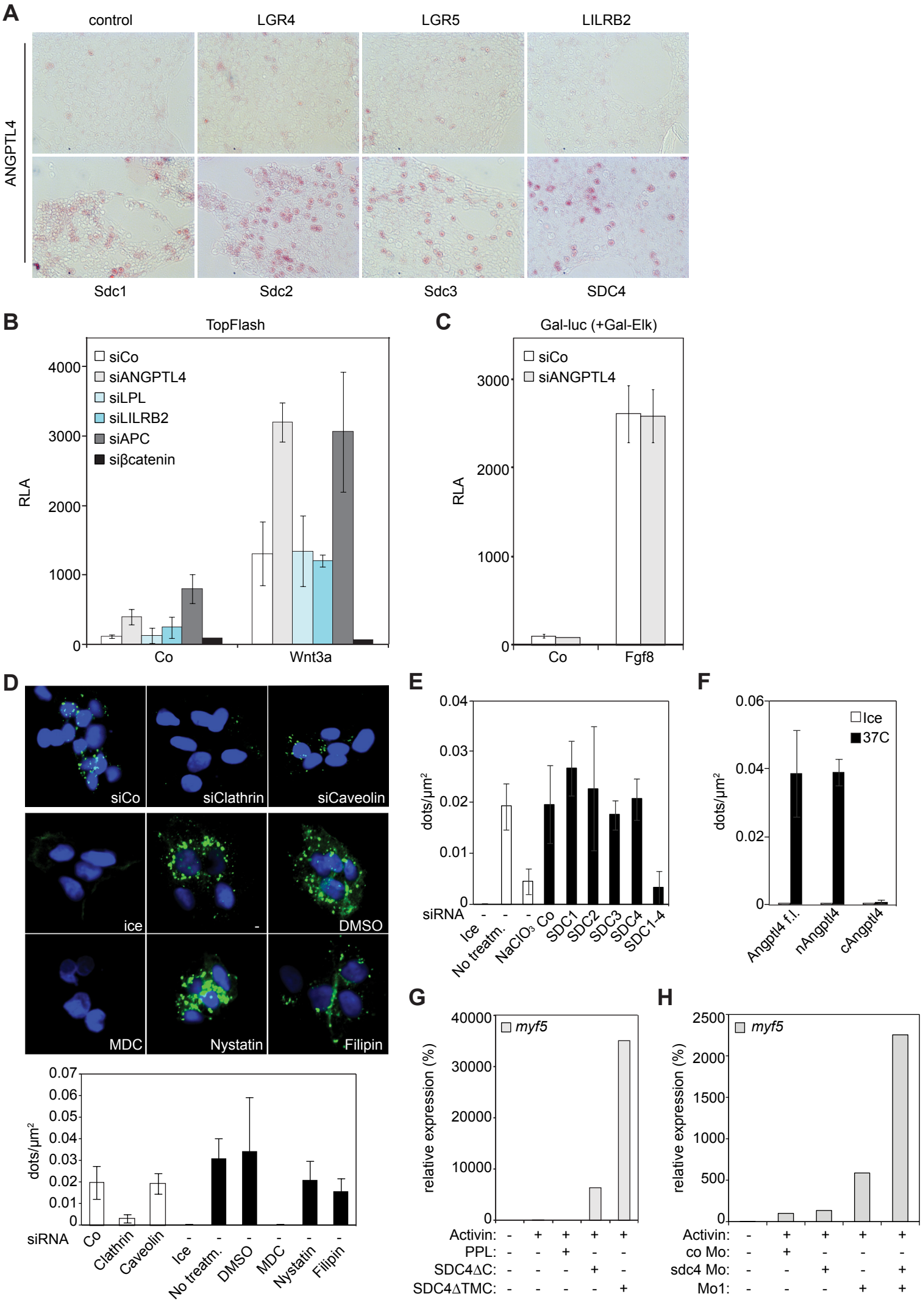
A
control
LGR4
LGR5
LILRB2
ANGPTL4
Sdc1
Sdc2
Sdc3
SDC4
B
TopFlash
siCo
siANGPTL4
siLPL
siLILRB2
siAPC
siβcatenin
RLA
Co
Wnt3a
C
Gal-luc (+Gal-Elk)
siCo
siANGPTL4
RLA
Co
Fgf8
D
siCo
siClathrin
siCaveolin
ice
-
DMSO
MDC
Nystatin
Filipin
dots/µm²
siRNA
Co
Clathrin
Caveolin
Ice
No treatm.
DMSO
MDC
Nystatin
Filipin
E
dots/µm²
siRNA
Ice
No treatm.
NaClO3
Co
SDC1
SDC2
SDC3
SDC4
SDC1-4
F
Ice
37C
dots/µm²
Angptl4 f.l.
nAngptl4
cAngptl4
G
myf5
relative expression (%)
Activin:
PPL:
SDC4ΔC:
SDC4ΔTMC:
H
myf5
relative expression (%)
Activin:
co Mo:
sdc4 Mo:
Mo1:

Figure S4, related to Figure 4. ANGPTL4 binds syndecans and is internalized by clathrin-dependent endocytosis.

(A) Cell surface binding assay in HEK293T cells. Cells were transfected with the indicated receptor constructs and incubated with conditioned medium containing ANGPTL4-AP (alkaline-phosphatase) fusion protein. Ligand binding was detected using a chromogenic AP substrate (red).

(B) Wnt luciferase reporter assay in H1703 cells in the presence of the indicated siRNAs.

(C) FGF reporter assay in HEK293T cells with binary Gal-Elk/Gal-luc reporter and stimulated with recombinant mFgf8. Data (B and C) are displayed as mean ± SD, with 3 biological replicates. Co, control. RLA, relative luciferase activity.

(D) Internalization assay in HepG2 cells. Cells were treated with the indicated siRNAs or endocytosis inhibitors, and incubated with HRP-tagged full-length ANGPTL4 (green). Protein internalization was detected by tyramide signal amplification. MDC, monodansylcadaverine.

(E, F) Quantification of the indicated internalization assays shown in Fig. 4C (E) and Fig. 4D (F). For internalization assays data are displayed as dots / μm^2 from multiple fields per condition. Data are displayed as mean ± SD.

(G, H) qRT-PCR analyses of *myf5* in animal cap explants from *X. tropicalis* embryos microinjected as indicated. Note that the experiments belong to the data shown in Fig. 4G and Fig. 4H respectively. Data show one representative of multiple independent experiments with at least 3 biological replicates each.

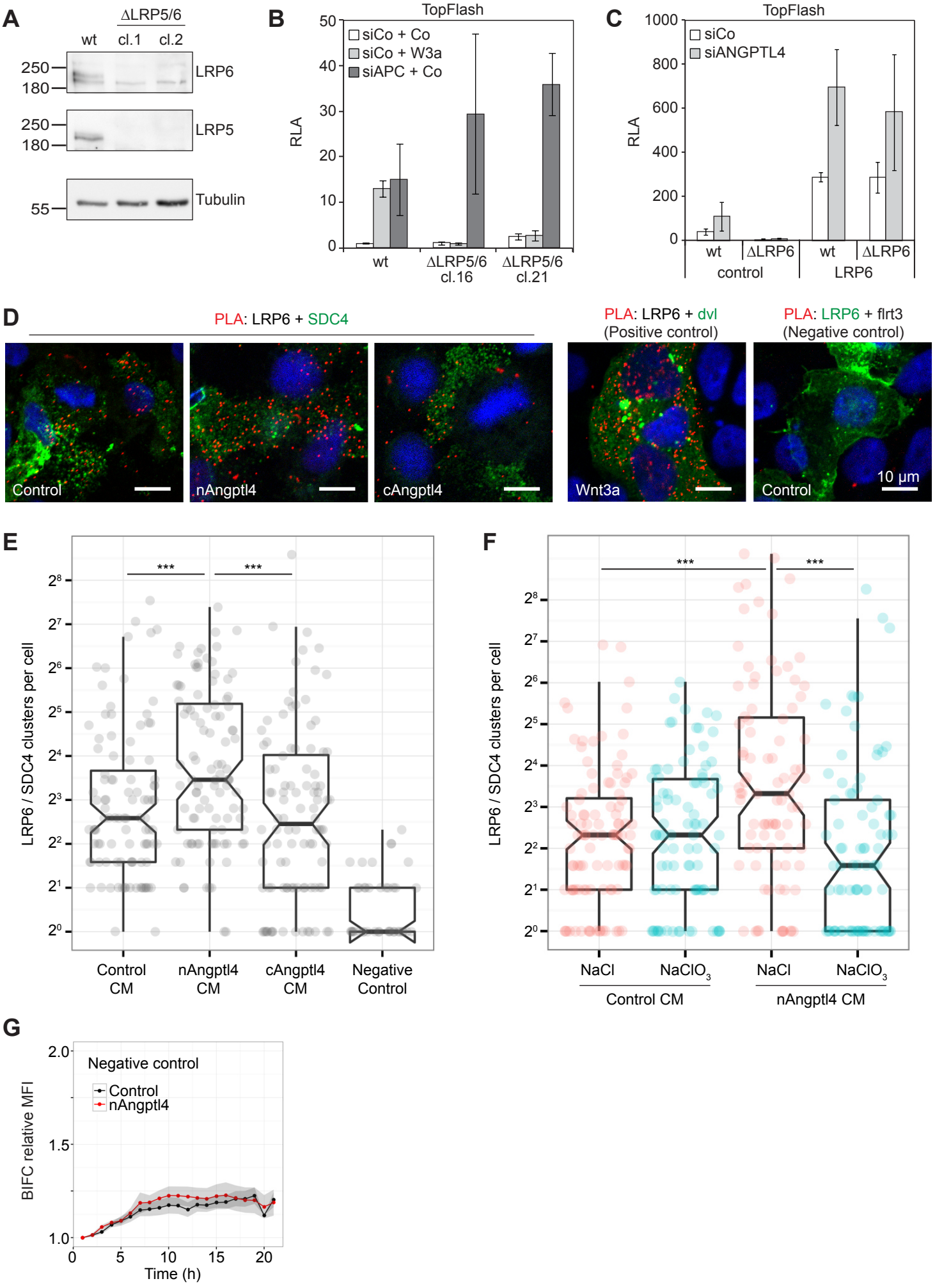
A
ΔLRP5/6
wt
cl.1
cl.2
250
180
LRP6
250
180
LRP5
55
Tubulin
B
TopFlash
siCo + Co
siCo + W3a
siAPC + Co
RLA
wt
ΔLRP5/6 cl.16
ΔLRP5/6 cl.21
C
TopFlash
siCo
siANGPTL4
RLA
wt
ΔLRP6
wt
ΔLRP6
control
LRP6
D
PLA: LRP6 + SDC4
PLA: LRP6 + dvl (Positive control)
PLA: LRP6 + flrt3 (Negative control)
Control
nAngptl4
cAngptl4
Wnt3a
Control
10 µm
E
LRP6 / SDC4 clusters per cell
***
***
Control CM
nAngptl4 CM
cAngptl4 CM
Negative Control
F
LRP6 / SDC4 clusters per cell
***
***
NaCl
NaClO3
NaCl
NaClO3
Control CM
nAngptl4 CM
G
Negative control
Control
nAngptl4
BIFC relative MFI
Time (h)

Figure S5, related to Figure 5. nAngptl4 promotes LRP6/SDC4 clustering.

(A) Characterization of HEK293T$^{\Delta LRP5/6}$ CRISPR/Cas9 cells by Western Blot. LRP5 and LRP6 protein were undetectable in two independent HEK293T$^{\Delta LRP5/6}$ clones compared to parental 293T cell line (wt).

(B) LRP5/6 knockout cells were completely unresponsive to Wnt stimulation in TopFlash assays, but retained functional β-catenin signaling, as evidenced by *APC* depletion.

(C) TopFlash assay in HEK293T parental and HEK293T$^{\Delta LRP6}$ cells. Re-expression of *LRP6* in LRP6 knockout cells restored sensitivity to ANGPTL4 depletion. Data (B and C) are displayed as mean ± SD, and show one representative of multiple independent experiments with 3 biological replicates. RLA, relative luciferase activity.

(D-F) Proximity ligation assay (PLA) in HEK293T$^{\Delta LRP6}$ cells. Cells transfected with V5-LRP6 and SDC4-eYFP were treated with the indicated conditioned media, and LRP6/SDC4 clustering was detected by proximity ligation. Representative images (D) and quantitative analysis (E) showed increased LRP/SDC4 cluster numbers following nAngptl4 treatment. (F) Inhibition of syndecan maturation by $NaClO_3$ blocked nAngptl4-induced LRP6/SDC4 clustering. Average cluster size in 100 cells per condition was determined by computer-assisted particle analysis. Data are displayed as box and whisker plots with median, interquartile range, and maximum/minimum values excluding outliers. Notches indicate the 95% confidence interval. Tukey's post-hoc test following one-way ANOVA was used for analysis.

(G) nAngptl4 has no effect on SDC4 - fibronectin leucine rich transmembrane protein 3 (flrt3) BIFC. For the bimolecular fluorescence complementation (BIFC) assay, cells were transfected with SDC4ΔC-C-Venus and flrt3ΔC-N-Venus and treated with Flag-nAngptl4 or control conditioned medium. Graphs show average relative MFI ± SEM (grey).

Table S1, related to Figure 4. Top hits of identified transmembrane or membrane attached interaction partners for ANGPTL4. ANGPTL4 pull-down was performed in HepG2 cells after addition of ProteinA_{x2}-TEV-Streptag-HRP-hANGPTL4 conditioned medium for 30 min. After a two-step pull-down process, purified samples were separated by SDS-PAGE and proteins stained with Coomassie Blue. Proteins pulled down with ANGPTL4 were analyzed by mass spectrometric analysis (ESI-MS/MS). Matrix proteins and proteoglycans were selected and sorted according to the number of unique peptides detected during MS analysis.

Accession No.	**Identified protein**	**#unique peptides**
ZO2_HUMAN	Tight junction protein ZO-2	17
FINC_HUMAN	Fibronectin	10
SDC4_HUMAN	Syndecan-4	4
LEG8_HUMAN	Galectin-8	5
SDC1_HUMAN	Syndecan-1	5
SDC2_HUMAN	Syndecan-2	3